Spatial Tessellations: Concepts and Applications of Voronoi Diagrams
Edition by ATSUYUKI OKABE & BARRY BOOTS and SUNG NOK CHIU

CHAPTER 7

Models of Spatial Processes

We have noted that the ordinary Voronoi diagram, $\mathcal{V}(P)$, of a set of n points, $P = \{p_1, \ldots, p_n\}$, in $\mathbb{R}^m$ is a tessellation of $\mathbb{R}^m$ since it consists of a set of regions that do not overlap, except possibly at their boundaries, and which completely cover $\mathbb{R}^m$ (see Section 2.3). Since there is a large number of empirical structures which also involve tessellations of $\mathbb{R}^m$, one of the most obvious direct applications of Voronoi concepts is in the modelling of such structures and the processes that generate them. Indeed, in Section 5.3 we have already shown how the Voronoi diagram associated with a set of points located in $\mathbb{R}^m$ according to the homogeneous Poisson point process (the Poisson Voronoi diagram) can be used as a normative model to evaluate and compare various empirical structures. In this chapter we take a more general approach which does not limit the location of the members of P to a particular spatial pattern and consider other processes which result in tessellations. We shall refer to these as models of spatial processes of which several different types are presented. In Section 7.1 we consider models involving spatial assignment processes while in Section 7.2 we consider models involving concepts of growth.

The models presented in both these sections assume that once formed the regions remain unchanged and that the phenomenon associated with the regions is of a single type or belongs to a single group. In Section 7.3 we relax the first assumption by permitting the regions to change in form after their initial creation. Since such situations involve an explicit time dimension, we refer to them as spatial–temporal processes. The second assumption is relaxed in Section 7.4 by considering situations in which regions are associated with different phenomena which compete for space (e.g. crops and weeds in a field, prey and predators in an ecosystem).

For convenience, throughout this chapter we refer to the tessellation of $\mathbb{R}^m$ associated with a particular phenomenon as a spatial pattern of that phenomenon. Also, since our concern is with modelling empirical structures, our treatment is limited to two- and three-dimensional Euclidean space.

7.1 ASSIGNMENT MODELS

These models describe processes which produce spatial patterns by allocating individual locations in $\mathbb{R}^m$ ($m = 2, 3$) or a bounded region in $\mathbb{R}^m$ (depending on the particular empirical circumstance) to a set of n points, $P = \{p_1, \ldots, p_n\}$, at positions $x_1, \ldots, x_n$, respectively, in the same space. If the following assumptions are made, the resulting set of regions is equivalent to the ordinary Voronoi diagram, $\mathcal{V}(P)$, of P:

Assumption VAM1 Each point, p_i ($i = 1, \ldots, n$), is located simultaneously before any assignment procedure occurs.

Assumption VAM2 Each point p_i remains fixed at x_i throughout the assignment process.

Assumption VAM3 Each point p_i is of equal importance.

Assumption VAM4 Each location which is closer in terms of Euclidean distance to p_i than to any other member of P is assigned to p_i; locations which are equidistant from two or more members of P are assigned to the boundaries of the regions of those points.

Collectively Assumptions VAM1–VAM4 define the *Voronoi Assignment Model.*

Given the simple assumptions of the Voronoi Assignment Model it is of no surprise that it has been evoked in a wide range of situations in an equally wide range of disciplines. One of the longer established areas of use is in modelling physical–chemical systems. Such systems are frequently considered to consist of a set of sites occupied by atoms, ions or molecules (depending on the specific application) which are represented as equal-sized spheres. When the sites are regularly arranged in $\mathbb{R}^m$, as they would be if they formed a lattice (see Figure 7.1.1(a)), then the structure is said to be *crystalline.* Such structures are also referred to as *periodic* or *ordered* since the physical situation at a given site is reproduced at other sites throughout the structure. Examples of such structures in $\mathbb{R}^m$ are encountered frequently in inorganic chemistry (Wells, 1984). When the sites are no longer regularly arranged but the radii of the spheres are not negligible relative to the average distance between sites, we have a structure such as that illustrated in Figure 7.1.1(b), which is referred to as an *amorphous* (alternatively *non-crystalline, non-periodic* or *disordered)* structure (Yonezawa and Ninomiya, 1983). In such structures the size of the spheres has an inhibitive effect on how closely the sites may approach each other (no closer than the diameter of the spheres). Consequently, although amorphous structures lack the long-range order of crystalline structures, they may still exhibit some degree of short-range (local) order. Examples of such structures include monatomic liquids and metallic glasses (Zallen, 1979). Finally, if the sites are not regularly arranged and the

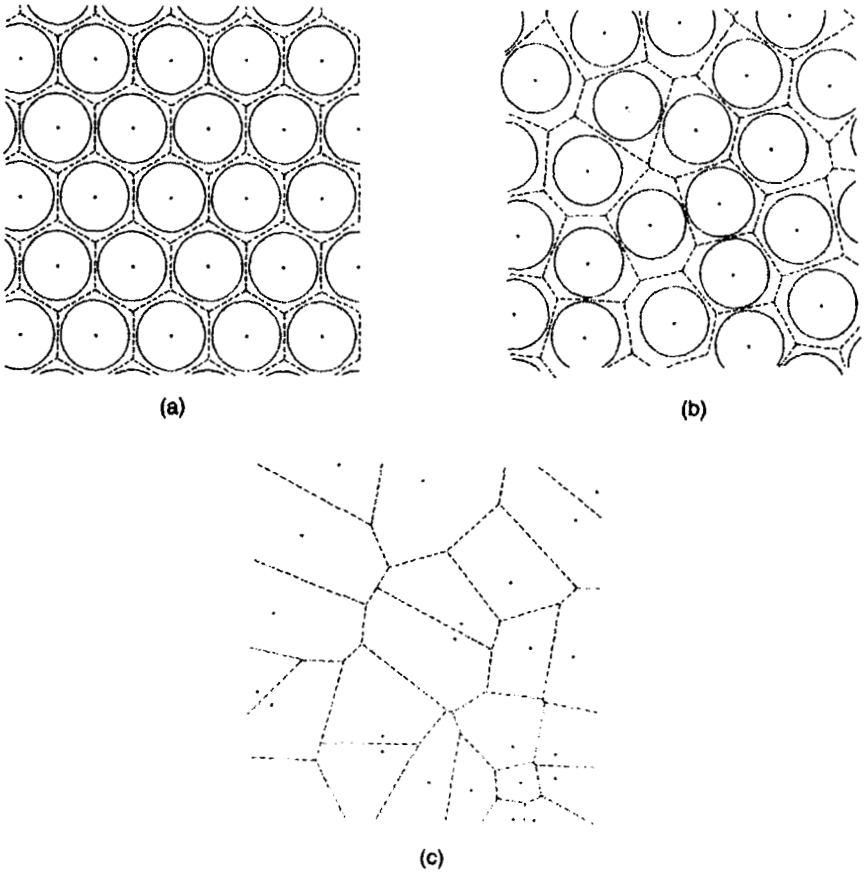

Figure 7.1.1 (a) Crystalline structure; sites and their associated spheres arranged on a lattice (dashed lines indicate Voronoi regions of sites). (b) Amorphous structure; sites and their associated spheres arranged irregularly (dashed lines indicate Voronoi regions of sites). (c) Ideal gas structure; sites located according to a homogeneous Poisson point process (dashed lines indicate Voronoi regions of sites).

radii of the spheres are considered negligible relative to the average inter-site distance, the inhibitive effect no longer occurs and the sites may occupy locations equivalent to those generated by a homogeneous Poisson point process (see Section 1.3.3) as shown in Figure 7.1.1(c). Such a structure is typical of many gasses and that in Figure 7.1.1(c) is often referred to as an *ideal gas* (Gil Montoro and Abascal, 1993). Both the crystalline and amorphous structures can thus be considered as consisting of closely spaced spherical atoms and it is in these situations that Voronoi concepts have been used extensively.

Regardless of how the sites are positioned in $\mathbb{R}^m$ it is possible to assign each location in $\mathbb{R}^m$ to the nearest site. The result is to produce the Voronoi diagram, $\mathcal{V}(P)$, of the sites (see Figure 7.1.1). Once this is done, the

characteristics of $\mathcal{V}(P)$ can be used to define various parameters of the atoms (ions, molecules) of the structure. One such property is the number of neighbours or *coordination number*, c_i, of the atom p_i which can be measured by the number of Voronoi regions adjacent to the Voronoi region, $V(p_i)$, of p_i (Frank and Kasper, 1958; Laves, 1967; Fischer and Koch, 1979; Allen *et al.*, 1983). The coordination number is considered a basic parameter on which many atomic properties, such as the atomic (ionic) radius, depend directly. The region with p_i as its centre and with vertices that are the sites whose Voronoi regions are adjacent to $V(p_i)$ is called the *coordination shell* (or *coordination polyhedron* in $\mathbb{R}^m$) of the site p_i (Frank and Kasper, 1958; Mackay, 1972; Loeb, 1976, p. 132). Examination of how the coordination polyhedra are connected together in space provides an alternative way of modelling the structure. However, for some amorphous structures, the coordination polyhedron of an individual atom p_i may include more distant members of P which are unlikely to interact with p_i. In such situations, various methods have been proposed for either weighting or discarding one or more faces of $\mathcal{V}(P)$ (Bernal, 1937; Brostow *et al.*, 1978; Hsu and Rahman, 1979b; O'Keefe, 1979; Medvedev, 1986; Rustad *et al.*, 1991a; Liška *et al.*, 1995a).

When the sites are regularly arranged they form a lattice. In this case each site has an identical environment in an identical orientation to every other site. More formally, in $\mathbb{R}^m$ a lattice consists of the set of points with position vectors, $\boldsymbol{p}$, of the form

$$\boldsymbol{p} = l_1\boldsymbol{a}_1 + l_2\boldsymbol{a}_2 + l_3\boldsymbol{a}_3 + \ldots + l_m\boldsymbol{a}_m\,, \tag{7.1.1}$$

where $\boldsymbol{a}_1, \boldsymbol{a}_2, \boldsymbol{a}_3, \ldots, \boldsymbol{a}_m$ are m linearly independent vectors and $l_1, l_2, l_3, \ldots, l_m$ are integers. A lattice is infinite. For lattices the Voronoi regions of the sites are identical parallelotopes, convex polytopes with pairs of mirror equal opposite faces which fill space by being juxtaposed in parallel orientation. The upper limit for the number of facets F of a Voronoi parallelotope is $F \leq 2(2^m - 1)$ (Minkowski, 1897). Fedorov (1885) was the first to note that there are two types in $\mathbb{R}^2$, the centrally symmetric convex hexagons and the

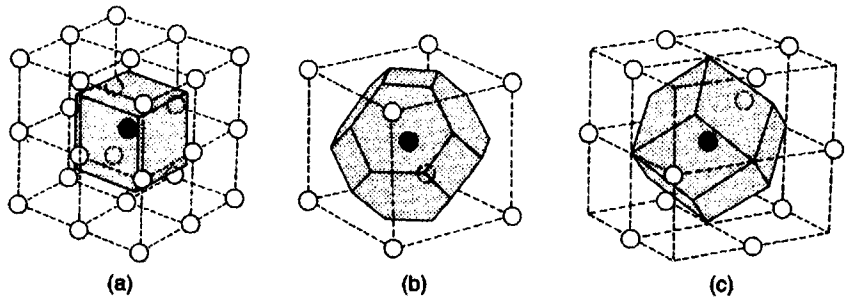

Figure 7.1.2 Some three-dimensional lattices and their associated Voronoi polyhedra: (a) simple cubic lattice, the Voronoi polyhedron is a cube: (b) body centred cubic lattice, the Voronoi polyhedron is a truncated octahedron; (c) face centred cubic lattice, the Voronoi polyhedron is a rhombic dodecahedron.

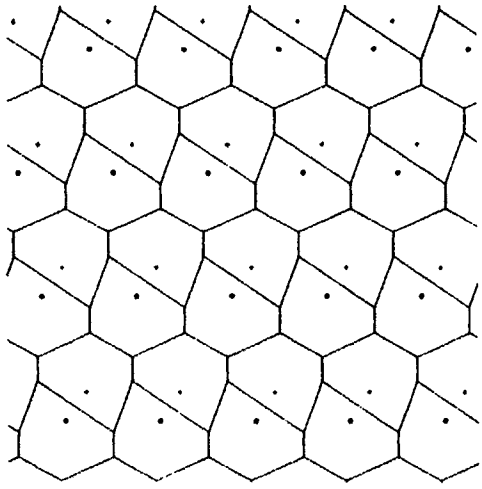

Figure 7.1.3 A lattice complex in $\mathbb{R}^2$ with sites of two different orientations.

parallelograms, and five in $\mathbb{R}^3$, the cube, hexagonal prism, rhombic dodecahedron, elongated dodecahedron, and truncated octahedron. Figure 7.1.2 shows the three types for which the corresponding point lattices are cubic. Forms with less symmetry can be obtained by distorting the basic five types by stretching or squeezing them along certain axes (Burzlaff and Zimmerman, 1977), yielding 24 classes of Voronoi regions (Bohm *et al.*, 1996). In $\mathbb{R}^4$ there are 52 types of Voronoi parallelotopes, 51 discovered by Delaunay (1929a, b) plus one more found by Stogrin (1973). The Voronoi region is also a primitive cell of the lattice. This is a bounded region which, when translated through all the vectors of the lattice, completely fills $\mathbb{R}^m$ without overlap except possibly at boundaries. Although there is no unique way of defining the primitive cell of a lattice, the primitive cell defined by the Voronoi region of a site has the advantage that it has the same degree of symmetry as the lattice.

In some crystal structures the sites are not arranged on a lattice. One possibility is that all sites are equivalent with respect to other point group operations, besides that of translation involved in a lattice, such as rotation about an axis or reflection. Such sites are said to form a *lattice complex*. In such cases the environments of the sites are identical except for orientation and the Voronoi regions are congruent but with more than one orientation. An example of a lattice complex in $\mathbb{R}^2$ where the sites are of two different orientations is shown in Figure 7.1.3. For lattices and lattice complexes in $\mathbb{R}^2$ all the different types of Voronoi polygons have been determined (Laves, 1930, 1931; Delone *et al.*, 1980; see Grünbaum and Shephard, 1987, Table 9.1.5, for a summary).

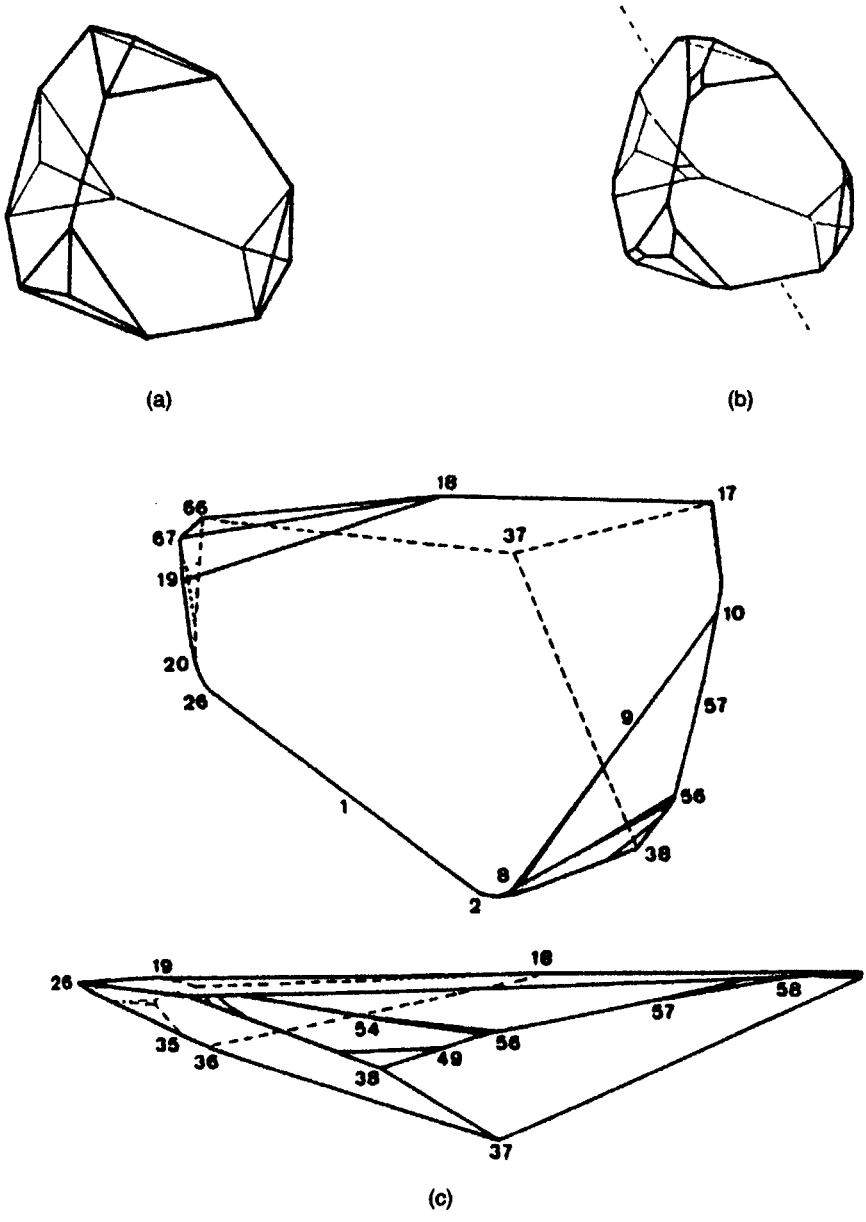

Figure 7.1.4 (a) 16-faced space-filling Voronoi region obtained from the 'diamond lattice'. (*Source*: Grünbaum and Shephard, 1980, Figure 8.) (b) 20-faced space-filling Voronoi region obtained from a distorted 'diamond lattice'. (*Source*: Grünbaum and Shephard, 1980, Figure 9(a).) (c) Two views of a 38-faced Voronoi region (some of the vertices are labelled to facilitate recognition. (*Source*: Engel, 1981, Figure 4.)

In $\mathbb{R}^3$ the Voronoi polyhedra are sometimes called *plesiohedra* (Grünbaum and Shephard, 1980). As such they are members of a larger set of regions of equal shape called *stereohedra*, congruent copies of any one of which are capable of filling $\mathbb{R}^3$ without overlap except possibly for boundaries. There has been considerable interest in crystallography in determining the maximum number of $(m-1)$-dimensional faces, F, of a stereohedron. Delone (1961) obtained the result that in m dimensions

$$F \leq 2^m(1+h)-2, \tag{7.1.2}$$

where h is the number of sets of sites with different orientations of their environments. For a lattice $h = 1$, and so for $\mathbb{R}^3$, expression (7.1.2) gives an upper limit of 14 which is achieved by the Voronoi polyhedra of a body centred cubic lattice. The Voronoi polyhedra are truncated octahedra with six square faces and eight regular hexagonal faces; all edges are of the same length (see Figure 7.1.2(b)). For $m = 3$ and $h = 2$ the upper limit of F given by expression (7.1.2) is 22. A stereohedron with this number of faces has not been identified but $F = 16$ for the lattice complex consisting of two interpenetrating face centred cubic lattices is usually referred to as the diamond structure (since the carbon atoms in a diamond crystal take on this arrangement) (see Figure 7.1.4(a)). A simplified version of this polyhedron has been used by Grigorovici and Manaica (1967/8) and Grigorovici (1969) as a model for germanium. Smith (1965) has identified stereohedra with 20 faces which are Voronoi polyhedra of a slightly distorted version of the diamond structure (see Figure 7.1.4(b)). Other examples of Voronoi polyhedra with 20 faces have been identified by Stogrin (1968, 1973). The upper limit of F for $m = 3$ is 390 since the maximum value for h in $\mathbb{R}^3$ is 48 (Henry and Lonsdale, 1965).

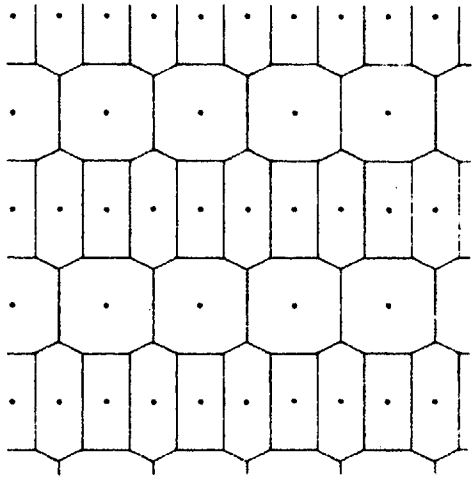

Figure 7.1.5 Voronoi diagram for sites belonging to three different sets of equivalent sites.

So far only a number of Voronoi polyhedra with 38 faces have been identified (Engel, 1981). One of these is illustrated in Figure 7.1.4(c). Other polyhedra with numbers of faces ranging from 17 to 37 have also been reported by a number of other researchers and these are reviewed in Grünbaum and Shephard (1980).

Conway and Sloane (1993, Chapter 21) extend the treatment of Voronoi regions for lattices in $\mathbb{R}^m$ ($m \geq 4$). Interestingly, the Voronoi diagrams of these and other periodic structures can also be used to generate quasi-periodic tessellations, such as Penrose tilings, in lower dimensional space (Kramer and Schlottmann, 1989; Baake *et al.*, 1990). Their method, the Klotz construction, exploits a generalization of the projection described in Property D8 (see Sections 2.4 and 3.1.4) so that the resulting quasi-periodic tessellations are Laguerre tessellations (Schlottmann, 1993) (see Section 3.5).

Another alternative to a lattice which is sometimes encountered in crystallography occurs when the sites are not equivalent with respect to one or more point group operations but instead belong to k different sets of equivalent sites. In such instances the Voronoi regions form k different sets of mutually equivalent regions which together fill $\mathbb{R}^m$. An example in $\mathbb{R}^2$ for $k = 3$ is illustrated in Figure 7.1.5.

The lack of regularity and homogeneity in amorphous structures means that there is a much greater need to be able to characterize such materials at the individual atomic (ionic, molecular) level than for crystalline structures (Turnball and Polk, 1972; Jerauld *et al.*, 1984a). Since such structures often are modelled initially as collections of randomly packed spheres (or discs in $\mathbb{R}^2$), a related conceptualization is to consider them as packings of polyhedra by defining the Voronoi diagram of the set of sphere centres (see Figure 7.1.1(b)). While earlier work focused on non-overlapping (hard), equal-sized spheres, models involving overlapping (soft) spheres and variable-sized spheres have been developed. In the latter instance, the power diagram or Laguerre Voronoi diagram (see Sections 3.1.4 and 3.5.3) (Mackay, 1981, 1983, 1986; Gellatly and Finney, 1982b, 1982c; Richards, 1985; Baranyai and Ruff, 1986; Mackay and Klinowski, 1986; Rivier, 1987, 1991, 1993; Finney, 1991, 1993; Gervois and Bideau, 1993; Annic *et al.*, 1994; Aparicio and Cocks, 1995; Van der Marck, 1996), the Voronoi diagram for a set of circles (spheres) (see Section 3.5.3) (Medvedev, 1994; Anishchik and Medvedev, 1995; Goede *et al.*, 1997) and the multiplicatively-weighted Voronoi diagram (see Section 3.1.1) (Gerstein *et al.*, 1995) have been suggested as being more appropriate than the ordinary Voronoi diagram. Another alternative, known as *Richards' method B* (Richards, 1974), is encountered in protein studies where it is considered to be a 'Voronoi procedure' (Chothia, 1975; Gellatly and Finney, 1982b; Harpaz *et al.*, 1994; Gerstein *et al.*, 1993, 1995; Gerstein and Chothia, 1996). However, since the polyhedra are constructed using planes which perpendicularly bisect the line segment joining two sphere centres in proportion to their respective radii, small, unallocated tetrahedrons are created near each polyhedral vertex so that the resulting structure is not a tessellation.

Others have suggested that it is preferable to represent such packings by means of the dual Delaunay tessellation (e.g. Smith, 1964; Ogawa and Tanemura, 1974; Finney and Wallace, 1981; Hiwatari *et al.*, 1984), especially if the focus of investigation is on the nature of the pore space within the packing rather than on the atoms themselves (Medvedev and Naberukhin, 1987b; Medvedev *et al.*, 1988, 1989, 1990; Voloshin *et al.*, 1989; Medvedev, 1990; Finney, 1991; Bryant and Blunt, 1992).

Voronoi polyhedral models have been extensively applied, especially in the study of liquids, glasses, and proteins. Illustrative studies of both general and specific kinds are summarized in Table 7.1.1.

Once a structure is represented as either a Voronoi diagram or a Delaunay tessellation, various metric and topological characteristics of the constituent polyhedra or simplices, or measures derived from them (Gervois and Bideau, 1993; Blatov *et al.*, 1995) can be used to differentiate between structures. For example, polyhedron (or tetrahedron) volume V and surface area S are frequently examined either individually (e.g. Rapaport, 1983; Schnitker and Mausbach, 1990; Gotoh, 1993; Finney, 1993; Gil Montoro and Abascal, 1993; Shih *et al.*, 1994; Niemelä *et al.*, 1996; Jund *et al.*, 1997) or jointly in dimensionless measures (Kimura and Yonezawa, 1984; Nose and Yonezawa, 1986; Rigby and Roe, 1990; Ruocco *et al.*, 1991; Gil Montoro and Abascal, 1993; Shih *et al.*, 1994). For Voronoi polyhedra, Ruocco *et al.* (1991) and Shih *et al.* (1994) suggest using an asphericity measure defined by

$$\eta = \frac{S^3}{36\pi V^2}. \tag{7.1.3}$$

The minimum value ($\eta = 1$) occurs for a sphere while values for the Voronoi polyhedra of the three cubic lattices discussed above are 1.33 (body centred cubic, truncated octahedron), 1.35 (face centred cubic, rhombic dodecahedron), and 1.91 (simple cubic, cube).

The topological characteristics of Voronoi polyhedra include the number of faces/polyhedron F, the number of edges/face N and the full topological index proposed by Finney (1970a) (see also Tanemura *et al.*, 1977; Hsu and Rahman, 1979b; Cape *et al.*, 1981; Bushnell-Wye *et al.*, 1982; Kimura and Yonezawa, 1984; Medvedev *et al.*, 1986; Medvedev and Naberukhin, 1987a; Watanabe and Tsumuraya, 1987; Rigby and Roe, 1990; Finney, 1993; Tsumuraya *et al.*, 1993; Blatov and Serezhkin, 1997). This involves describing the local configuration of an atom a_i, with associated Voronoi polyhedron, $V(a_i)$, with f_i faces, by listing the number of faces, $n_3, n_4, n_5, \ldots, n_j$, having $3, 4, 5, \ldots, j$ edges, where $\sum_{k=i}^{j} n_k = f_i$. Re-analysis of previously published results relating to argon (Rahman, 1966; Finney, 1970b; Tanaka, 1986b; Medvedev and Naberukhin, 1987a), rubidium (Tanaka, 1986a), and supercooled water (Ruocco *et al.*, 1991) led Kumar *et al.* (1997) to propose using the coefficient of variation of F as a descriptor of topological disorder which is particularly effective in studying solid–liquid–glass transitions.

For Delaunay simplices, measures such as volume (Voloshin *et al.*, 1989), circumradius (Hitawari *et al.*, 1984; Medvedev and Naberukhin, 1987b;

Table 7.1.1 Studies involving Voronoi diagrams of packing of spheres.

Application	Disc(2)/sphere(3)	hard(h)/soft(s)	equal(e)/variable(v)	Reference
General	2/3	h	e	Ogawa and Tanemura (1974)
	3	h	e/v	Medvedev (1994)
Dense packings	3	h	e	Bernal and Finney (1967)
	3	h/s	e	Medvedev and Naberukhin (1987b)
Lower density random packings	3	h	e	Bernal and King (1967)
Different random configurations	2	h	e	Gotoh (1993)
Air cushion table	2	h	e	Lemaitre *et al.* (1991, 1993)
				Gervois *et al.* (1992)
	2	h	v	Lemaitre *et al.* (1992)
				Annic *et al.* (1994)
Porous media	2	h	e	Chan and Ng (1988)
				Vrettos *et al.* (1989a)
	3	h	e	Roberts and Schwartz (1985)
				Vrettos *et al.* (1989b, 1990)
				Bryant and Blunt (1992)
Percolation	3	s	e	Kerstein (1983)
	3	s	v	Van der Marck (1996)
Hollow fibre modules	2	h	e	Chen and Hlavacek (1994)
				Rogers and Long (1997)
Ostwald ripening	2	h	e	Masbaum (1995)
Crystallization	3	h	e	Hsu and Rahman (1979b)
	3	s	e	Tanemura *et al.* (1977)
	3	s	e	Cape *et al.* (1981)
Melting	2	h	e	McTague *et al.* (1980)
				Weber and Stillinger (1981)
				Allen *et al.* (1983)
	3	h	e	Hsu and Mou (1992)
Entropy of melting	3	h	e	Rivier and Duffy (1982)
Liquids	3	h	e	Kimura and Yonezawa (1984)
				Medvedev *et al.* (1988, 1989)
				Gil Montoro and Abascal (1993)
Monatomic liquids	3	h	e	Bernal (1959, 1964)
	3	h	e	Smith (1964)
	3	h	e	Collins (1967)
	2/3	h	e	Collins (1968, 1972)
	3	h/s	e	Finney (1970a,b)
	3	h	e	Brostow and Sicotte (1973)
High density liquids	3	h	e	Krishnamurthy *et al.* (1988)
	2	h	e	Glaser and Clark (1990)
Supercooled liquids	3	s	e	Tanemura *et al.* (1977)
Liquid water	3	h	e	Schnitker *et al.* (1986)
				Schnitker and Mausbach (1990)
				Shih *et al.* (1994)
Liquid water, liquid hydrogen sulphide	3	h	e	Ruocco *et al.* (1991)
Supercooled water	3	h	e	Rapaport (1983)
Mobility of stretched SPC/E water	3	h	e	Vaisman *et al.* (1993)
Pure dimethylsulphide (DMSO), water–DMSO mixtures	3	h	e	Vaisman and Berkowitz (1992)
Electrolyte solutions	3	h	e	Gil Montoro *et al.* (1994)
Lennard-Jones system (argon)	3	h/s	e	Barker *et al.* (1975)
				Medvedev *et al.* (1986)
				Nose and Yonezawa (1986)
				Medvedev and Naberukhin (1987a)
				Medvedev *et al.* (1988, 1989)
				Voloshin *et al.* (1989)

Table 7.1.1 *cont.*

Application	Disc(2)/sphere(3)	hard(h)/soft(s)	equal(e)/variable(v)	Reference
Liquid argon	3	h	e	Brostow and Sicotte (1975) Tanaka (1986b)
Liquid and crystalline argon	3	h	e	Galashev and Skripov (1980)
Liquid and quenched rubidium	3	h	e	Hsu and Rahman (1979a,b) Tanaka (1986a,b) Medvedev (1990) Medvedev *et al.* (1990)
Molten rubidium chloride, lithium iodide	3	h	v	Baranyai and Ruff (1986)
Molten cryolite (Na_3AlF_6)	3	h	e	Liška *et al.* (1995)
Crystallization and glass formation in liquid sodium	3	h	e	Watanabe and Tsumuraya (1987)
Liquids and glasses	3	h	e	Finney (1975a)
Rapidly quenched liquids and glasses	3	h/s	e	Hitawari *et al.* (1984)
Polymer liquid and glass	3	h	e	Rigby and Roe (1990)
Glassy polysulfones	3	h	e	Niemalà *et al.* (1996)
Glasses	3	h	e	Rivier (1983a, 1985b)
Metallic glass	3	s	e	Finney and Wallace (1981)
	3	h	e	Rivier (1987)
	3	h	e	Troadec and Dodds (1993)
Pd_4Si	3	h	v	Gellatly and Finney (1982c)
Silicon glass	3	h	e	Tsumuraya *et al.* (1993)
Amorphous silicon or germanium	3	h	e	Krishnamurthy *et al.* (1988)
Amorphous silica	3	h	e	Rustad *et al.* (1991a,b)
Calcium aluminosilicate glasses	3	h	e	Liška *et al.* (1995)
Glass transition	3	h	e	Jund *et al.* (1997)
Granular media	2	h	e/v	Gervois and Bideau (1993)
Sintering of fine particles	3	h	e/v	Aparicio and Cocks (1995)
Densification of powders by cold compaction, hot-isostatic pressing and sintering	3	h	e	Arzt (1982)
Zirconia nanocrystals	3	h	v	Ogawa *et al.* (1996a, 1997)
Al-10% (by weight) Si binary alloy	2	h	e	Brockenbrough *et al.* (1992)
Pd-Si alloys	3	h	e	Ohkubo and Hirotsu (1996)
$Cu_{57}Zr_{43}$ alloy	3	h	e	Kobayashi *et al.* (1980)
Proteins	3	h	e	Chothia (1975) Finney (1975b) Pontius *et al.* (1996)
Globular proteins	3	h	e	Finney *et al.* (1980)
Lysozyme and ribonuclease S	3	h	v	Richards (1974) Finney *et al.* (1980)
Ribonuclease S	3	h	e	Finney (1978)
	3	h	e/v	Gellatly and Finney (1982b)
Myoglobin	3	h	e	Procacci and Scateni (1992)
	3	h	v	Richards (1979)
Pancreatic trypsin inhibitor	3	h	v	Richards (1979) Finney *et al.* (1980) Gerstein *et al.* (1995) Goede *et al.* (1977)
Lactoferrin	3	h	v	Gerstein *et al.* (1993)
Protein–water interface	3	h	v	Gerstein and Chothia (1996)
Protein folding	3	h	v	Harpaz *et al.* (1994)

Note: Studies categorized as involving equal (e) spheres include those which recognize more than one type of sphere but which do not take this into account in constructing the Voronoi diagram (i.e. the ordinary Voronoi diagram is used rather than a generalized Voronoi diagram).

Voloshin *et al.* 1989; Medvedev *et al.*, 1990), edge lengths (Hiwatari *et al.*, 1984; Nose and Yonezawa, 1986; Finney, 1993; Masbaum, 1995), and solid angles (Kimura and Yonezawa, 1984) can be used. For instance, Hiwatari *et al.* (1984) propose characterizing the shape of a Delaunay simplex using an irregularity parameter

$$\delta = \frac{1}{6\bar{l}} \sum_{i=1}^{6} |l_i - \bar{l}|, \tag{7.1.4}$$

where l_i is the length of the ith edge, and $\bar{l}$ is the average edge length of the given simplex. However, since analyses of computer models of dense random packings of monotonic systems of spheres show that most Delaunay simplices are close in shape to either the perfect tetrahedron or a quarter of a perfect octahedron (Finney and Wallace 1981), Medvedev *et al.* (1988, 1989) (see also Medvedev and Naberukhin, 1987a,b; Voloshin *et al.*, 1989; Medvedev, 1990; Medvedev *et al.*, 1990; Vaisman and Berkowitz, 1992; Vaismann *et al.*, 1993, 1994) suggest focusing on measures such as

$$T = \frac{1}{15\bar{l}^2} \sum_{i>j} (l_i - l_j)^2 \tag{7.1.5}$$

and

$$O = \frac{1}{10\bar{l}^2} \sum_{i>j\, i,j\neq m} (l_i - l_j)^2 + \frac{1}{5\bar{l}^2} \sum_{i\neq m} \left(l_i - \frac{l_m}{\sqrt{2}} \right)^2, \tag{7.1.6}$$

where l_m is the length of the maximum edge of the given simplex, which for an ideal octahedral simplex is $\sqrt{2}$ times longer than the rest of the equal edges. For a perfect tetrahedron $T = 0$, while $O = 0$ for a perfect octahedron.

In packings of hard spheres the proportion of the volume of the structure contained within the spheres is referred to as the *atomic volume* or the *packing fraction* of the material, or the *density of the packing*. A long believed but still unproven conjecture holds that the densest packing of equal sized spheres in $\mathbb{R}^3$ occurs when the sphere centres form a face centred cubic lattice (density $= \pi/\sqrt{18} = 0.74048$). In other situations it may be possible to increase the packing fraction of the initial packing. One way of doing this is to expand each sphere within the Voronoi region defined by its centre until the sphere touches one or more of the faces of the Voronoi region. Of course, the sizes of the resulting spheres are no longer equal. Anishchik and Medvedev (1995) present a more general sequential procedure for progressively increasing the packing fraction of variable-sized spheres. At each step, the locations of the centres of the new spheres are determined by the Voronoi vertices of the Voronoi diagram of existing spheres. Bieshaar *et al.* (1995) use a similar procedure to identify suitable locations to insert a non-overlapping test particle to calculate the excess chemical potential of a system of interacting particles. If the particles are represented by equal-sized spheres, each Voronoi vertex is simultaneously the circumcentre of the Delaunay simplex associated with the vertex and the centre of the largest sphere which can be inscribed inside the four spheres whose centres are the vertices of the

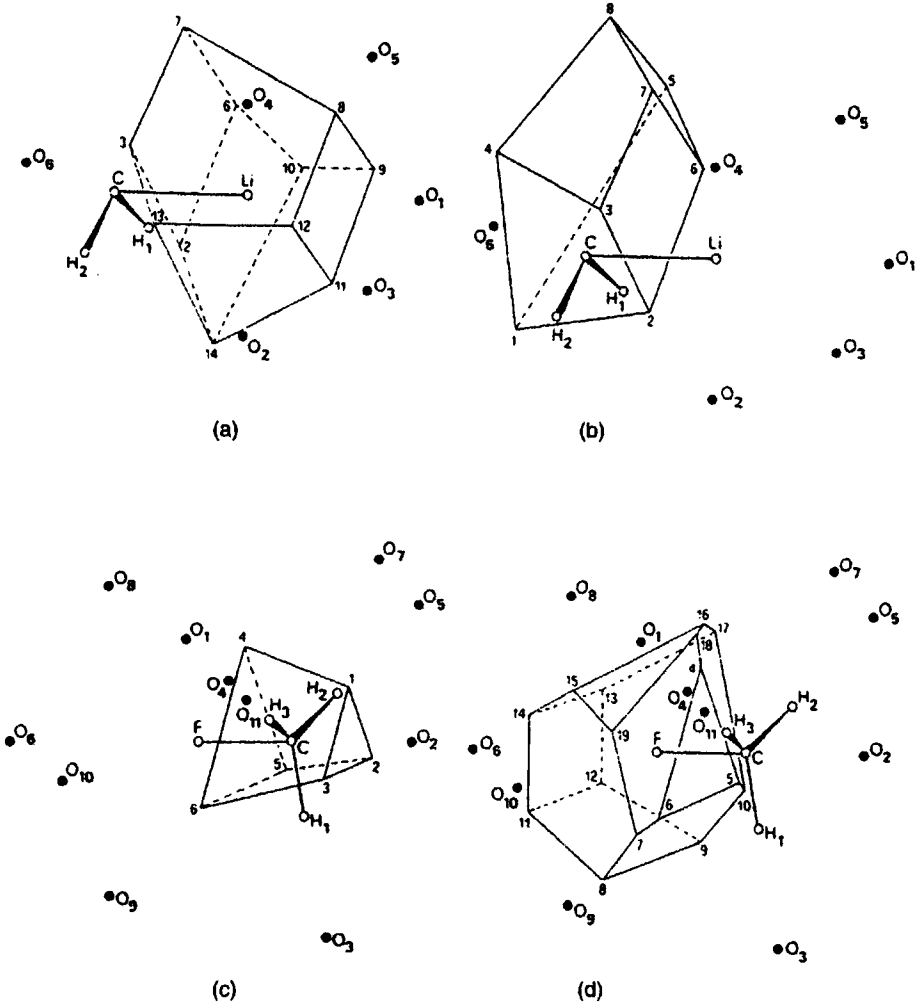

Figure 7.1.6 Voronoi polyhedra for different types of atoms in solvation structures: (a) lithium and (b) carbon atoms for $CH_2Li^+(H_2O)_6$; (c) carbon and (d) fluorine atoms for $CH_3F(H_2O)_{11}$. Filled circles represent the positions of oxygen atoms of water molecules. (*Source*: Bellagamba *et al.*, (1985, Figures 1 and 4.)

Delaunay simplex (Medvedev, 1994). Such locations are selected as test sites provided that there is sufficient free volume in the Delaunay simplex in which to insert a spherical test particle.

In Voronoi diagrams defined for centres of unit circles in the plane, the smallest Voronoi polygon is the regular hexagon and the smallest n-sided Voronoi polygon ($n \leq 6$) is a regular n-gon (superscribing a unit circle) with an area, a_n, of $n \tan(\pi/n)$. For $n > 6$, the smallest n-sided Voronoi polygon is not regular and there is no known formula for a_n. However, Muder (1990)

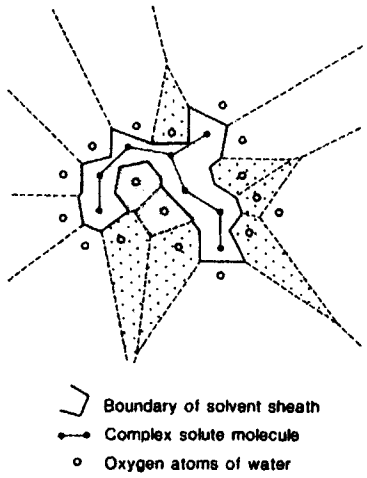

Figure 7.1.7 Identification of solvent accessible cleft regions of a solute. Stippled areas indicate molecules on the dimple region of the solvent; cross-hatched areas indicate molecules occupying a true cleft.

derives expressions for the upper and lower bounds on a_n from which he concludes that $a_n/n \to 1/\pi$. For packings of equal spheres in $\mathbb{R}^3$, it is widely believed, but not proven, that the smallest Voronoi polyhedron is the regular pentagonal dodecahedron, although such polyhedra are incapable of filling space. Muder (1988) proves that the optimal face of a Voronoi polyhedron is a regular pentagon slightly smaller than the faces of the regular dodecahedron. He also shows that for the packing density to be maximized, the best three- and four-sided faces are regular triangles and quadrilaterals, respectively.

The Voronoi concepts used above to study monatomic liquids have also been extended to non-monatomic ones. One instance is the modelling of solution structures consisting of a combination of a solvent and a solute, with particular attention being given to aqueous solutions. Initially, David and David (1982b) proposed constructing the Voronoi polyhedron of each atom of the solute using the oxide anions of the solvent water and the other atoms of the solute. Later they extended the construction of the Voronoi polyhedra to include the protons of the solvent as well (David and David, 1982c). Once defined, the Voronoi polyhedra of the atoms of the solute can be used in a variety of ways. First, the union of the polyhedra of the atoms of the solute can be considered to be the *solvent sheath* (i.e. the region that contains the solute as its interior region) (see Figure 7.1.7). The volume of the solvent sheath so defined can be considered to be the co-volume of the solvent as measured by water while the area of its external faces measures the extent to which each solvent molecule coordinates each atom of the solute (David and David, 1983; Bellagamba *et al.*, 1985). The properties of

different solvents can be studied by examining the corresponding solvent sheaths (Bellagamba *et al.*, 1985) or differences in the shapes and volumes of the Voronoi polyhedra of the solute atoms (Bellagamba *et al.*, 1986). Figure 7.1.6 shows the Voronoi polyhedra for the different types of atoms for two different solvation structures.

The Voronoi diagram can also be used to divide the solvent into subsets. For example, in their study of highly polar fluids, Neumann *et al.* (1978, 1979) use Voronoi polyhedra to define two concentric regions around a giant diopole. Similarly, Abseher *et al.* (1996) investigate the influence exerted by the globular protein ubiquitin on the solvent dynamics in its vicinity using three subsets: a first solvation shell (equivalent to the solvent sheath), a second solvation shell consisting of the Voronoi polyhedra surrounding the first hydration shell, and the remaining bulk. Vaisman *et al.* (1994) establish a similar division when they use T, the tetrahedrality measure for Delaunay simplexes described in equation (7.1.5), to show how the structure of water changes with distance from methane and ammonium ions.

David and David (1982a) also propose using the Voronoi construction to determine if a given atom is a member of a set of solute atoms forming a single cluster in a solvate. An atom is considered to be a cluster member only if its Voronoi polyhedron, as defined using the other atoms of the set and the atoms of the solvent, is closed. David (1984) also suggests that the solvent accessible cleft regions of a solute can be identified using Voronoi concepts. The approach is illustrated in Figure 7.1.7, which for convenience shows a two-dimensional representation of a complex of solute molecules (shown by filled circles) solvated by water molecules (shown by unfilled circles). The union of the Voronoi polygons of the solute atoms constitutes the solvent sheath. If we consider the Voronoi polyhedra of the water molecules which are adjacent to the solvent sheath we observe that these may be either open or closed. The open Voronoi polygons can be considered as the surface solvating water molecules while the closed Voronoi polygons are of two types. Some (those shown stippled in Figure 7.1.7) exist because the molecule is, at least partially, on the dimple region of the solvent while others (those shown cross-hatched in Figure 7.1.7) occupy a true cleft of the solute molecules. Such clefts represent regions where solute molecules may come into contact as a result of the elimination of the intervening solvent. David (1986) suggests that this touching, the so-called 'docking problem' of biology, can be recognized when one or more of the faces of the Voronoi polyhedra of the solute molecules are shared with those of polyhedra of other solute molecules. This procedure is implemented in an application involving the insertion of a NAM–NAG–NAM molecule in the cleft of hen egg white lysozyme (David, 1988b). Lewis (1989) also uses clefts defined by the Voronoi diagram of the centres of atoms of a receptor to identify putative binding sites for use in computer-aided drug design.

Drug design is one instance of the more general problem of understanding the specific binding of small molecules to biological receptors. In this context Crippen and his associates (Crippen, 1984, 1987, 1995; Boulu and Crippen,

1989; Boulu *et al.*, 1990) have developed and refined a *Voronoi site model.* Given the observed binding energies for a series of compounds, the goal of the model is to attempt to deduce the structure and energies of a binding site. Specifically, the atoms of a ligand molecule are represented as a collection of points in space, and site geometry is modelled as the Voronoi regions of a set of generating points supplied by the investigator. Thus, every atom of the ligand molecule lies in one and only one Voronoi region and the orientation and internal configuration of a particular binding mode can be expressed by stating the Voronoi region in which each atom is found. Whenever a ligand atom lies in a Voronoi region of a site it is considered to be in contact and the contact makes an additive contribution to the total binding energy. Once all geometrically and conformationally allowed binding modes are identified, solutions with the minimal number of site points which simultaneously offer the greatest number of energetically satisfactory binding modes allowed for each molecule are searched for. Applications of the model to investigations of binding include studies of cocaine analogues at the cocaine receptor sites on the dopamine transport system (Srivastava and Crippen, 1993; Crippen, 1995), triazines and pyrimidines to *L. casei* dihydrofolate reductase (Bradley and Crippen, 1993), and steroid molecules to corticosteroid and testosterone-binding human globulin (Schnitker *et al.*, 1997).

Voronoi concepts have also been used extensively in modelling metallurgical structures. This is because one prevalent approach used in quantitative metallography involves the identification of microstructural characteristics, their measurement, and the deduction of empirical relationships linking these characteristics to the physical and mechanical properties of the material (Lantuejoul, 1980; Burger *et al.*, 1990). Furthermore, many of the processes which affect such structures operate at the local level. Examples include competition between heterogeneous flow and decohesion and the development of recrystallization nuclei during plastic flow (Burger *et al.*, 1988). In particular, the Voronoi Assignment Model has been employed to characterize the structure of second-order particles in metals by considering the particles as points and defining their Voronoi diagram (Wray *et al.*, 1983; Koken *et al.*, 1988; Stone and Tsakiropoulos, 1995). Examples include sulphide inclusions and carbides in steels and graphite fibres in aluminium (Spitzig *et al.*, 1985) and non-metallic inclusions in Ti–V microalloyed steel under different conditions (Shehata and Boyd, 1988; Vander Voort, 1992). Pyrz (1994) uses the same approach to analyse the distribution of fibres in a glass/epoxy composite.

Another metallurgical application is involved in modelling the accumulation of structural damage in materials subjected to stress at elevated temperatures. In such situations, voids which nucleate on grain boundaries grow and subsequently coalesce causing fracture. One input parameter required by void growth models developed so far is the area, A_i, of the grain boundary affected by a given void, v_i, over which local stress occurs. Wilkinson (1988a, b) used the area of the Voronoi polygon of v_i as a measure of A_i.

The Voronoi Assignment Model has also been used in studies of submonolayer film growth, such as the epitaxial growth of semiconductors and metals and the non-epitaxial growth of metals on amorphous substrates. Here growth theories define initial regions in which the density of isolated atoms on the surface, called monomers, increases linearly with time until small islands begin to nucleate. As deposition continues, the density of the islands eventually exceeds that of the monomers. The process then enters an aggregation phase during which diffusing monomers are captured by existing islands. This process terminates once the islands start to coalesce. Following initial work by Venables and Ball (1971), Mulheran and Blackman (1995, 1996) and Blackman and Mulheran (1996) suggest that during the aggregation phase, the region from which an island acquires the monomers responsible for its growth, i.e. its capture zone, can be modelled by a Voronoi cell of the island. The particular form of the cell depends on whether the growth process is considered to be heterogeneous or homogeneous. In the former instance, the island can be represented by a central point and the ordinary Voronoi diagram is constructed, while in the latter it is represented as a circle whose radius is proportional to the number of monomers it has absorbed and the Voronoi diagram for a set of circles is constructed (see Section 3.5.3).

Ever since Honda *et al.* (1979) and Saito (1982) observed that Voronoi polygons closely approximate a variety of monolayer cells and epithelial cells in tissue, the Voronoi Assignment Model has been used increasingly in such applications. For example, Roudot *et al.* (1990) use the Voronoi diagram as the basis of a model of apple tissue while Weliky and Oster (1990) use it to determine the initial configuration of cell shapes and sizes in a model of morphogenesis in epithelial sheets. However, most applications involve animal and human tissues. These include modelling the distribution of both capillaries and fibres in transverse sections of muscle tissue. In the former, Voronoi polygons (here referred to as *capillary domains*) are defined with respect to capillaries represented as points (Hoofd *et al.*, 1985; Egginton *et al.*, 1988; Egginton and Ross, 1989b; Batra and Rakusan, 1991). Adjacencies of the Voronoi polygons in the resulting Voronoi diagram provide identification of neighbouring capillaries. A mean inter-capillary distance can then be defined for neighbouring capillaries which is a basic input parameter in models of oxygen transport in tissues (Egginton and Ross, 1989a; Egginton *et al.*, 1987). In this instance, the assumptions involved in the Voronoi Assignment Model are equivalent to assuming that the capillaries possess equal transport capacity and that they have equal levels of partially pressurized oxygen (Egginton, 1990). Thus, the models are most appropriate for muscle consisting of a single fibre type such as cardiac muscle (Turek *et al.*, 1986) and skeletal muscle for fish (Egginton *et al.*, 1987). Egginton (1990) provides a comprehensive review of this area of application.

Two types of fibre (slow-twitch and fast-twitch) occur within muscles and their spatial arrangement is considered to be an indicator of possible abnormalities. To follow this line of investigation it is necessary to determine which

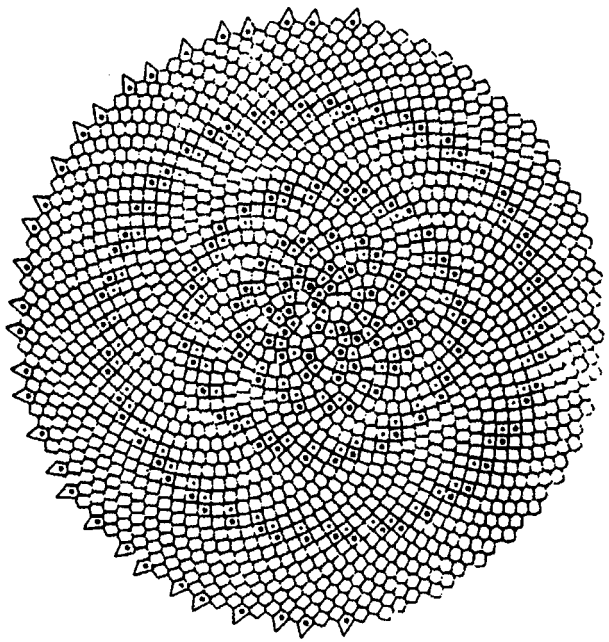

Figure 7.1.8 Simple daisy structure. (*Source*: Rivier *et al.*, 1984, Figure 6.)

fibres are neighbours. If the muscle fibres are represented as points located at fibre centroids, Paton and Zucker (1983) suggest that the Gabriel graph (see Section 2.5) be used to define neighbours, while Pernus (1988) proposes a spectrum of graphs which has the Gabriel graph and the Delaunay tessellation as its limits (see Section 8.4.2). Alternatively, Venema (1991) represents each fibre as a circle of equivalent area centred on the fibre centroid and uses the adjacency relationships in the power diagram (see Section 3.1.4) to define neighbours. Another possible indicator of abnormality is fibre shape, with healthy fibres being approximately hexagonal. Thus, Taylor *et al.* (1995) and Dryden *et al.* (1997) suggest generating the Delaunay triangulation of the fibre centroids and examining the degree to which the resulting triangles depart from equilateral ones (see Section 8.2).

Similar procedures have been used to investigate cancer cells. In a study of primary lung carcinoma, Kayser and Stute (1989) construct the Voronoi diagram of the geometric centres of cell nuclei in sections of surgical lung specimens and show that properties of the Voronoi polygons can be used to separate benign from malignant adenomatous tumours. Darro *et al.* (1993) use Voronoi diagrams defined in the same way to model the cell dynamics of human LOVO and HCT-15 colorectal neoplastic cell colonies growing in histological slides. Famiglietti (1992) also uses Voronoi polygons as one means of assessing the influence of the structural organization of Type 1 polyaxonal (PA1) amacrine cells in rabbit retina on their possible functionality.

We have already noted the use of Voronoi Assignment Models in studying periodic structures in chemistry. They have also been used in modelling a different type of periodicity which occurs in biology in phyllotaxis, the spiralling close packed arrangement of florets in composite plants such as daisies, asters and sunflowers and the scales of a pine cone or pineapple where successive florets are either identical or have a structure which can be obtained from the previous one. Rivier (1986c, 1988) and Rivier *et al.* (1984) have modelled the individual florets as Voronoi regions created with respect to points located on a parabolic spiral. Label the individual florets with positive integers ($i = 1,2,\ldots$) with the magnitude of the integer reflecting the age of the floret. If the stem is the origin of the coordinate system, the polar coordinates (r_i, θ_i) of the generator point of a floret are $r_i = ai^{1/2}$ and $\theta_i = 2\pi\alpha i$, where a is the average linear dimension of a floret (with area πa^2) and α $(0 < \alpha < 1)$ is a parameter of the structure. Thus, the florets are generated at regular intervals from the stem and at a given angle $2\pi\alpha$ from each other. Rivier *et al.* (1984) and Rivier (1986c, 1988) prove that, in order to create florets which are as uniform as possible in terms of size and shape (expressed by the number of edges of the floret), α must be an irrational number (rational α produces a spider web-like structure) of the form

$$\alpha = 1\{q_1 + 1/[\,q_2 + 1/(q_3 \ldots)]\},$$

where q_j are positive integers. The simplest solution occurs when $q_j = 1$ for all j and $\alpha \simeq 0.618$ which is also equal to the reciprocal of the golden mean $([1 + \sqrt{5}]/2)$. This structure is illustrated in Figure 7.1.8.

There is also extensive use of the Voronoi Assignment Model in both plant and animal ecology. Indeed, this application represents yet another area in which Voronoi polygons were discovered independently; not once but twice! Brown (1965) defined what he called the *area potentially available* (*APA*) to a plant which, as Jack (1967) recognized, is equivalent to the Voronoi polygon of the plant. Later Mead (1966, 1967, 1971) defined the same region labelling it the *plant polygon*. The polygon adjacencies in the Voronoi diagram of a set of plants (or trees) are used to define the neighbours of a given plant (Reed and Burkhart, 1985; Kenkel *et al.*, 1989), while the Voronoi polygon associated with an individual plant is considered an indicator of the portion of the environment available to that plant. Since interactions between plants are localized, the characteristics of the Voronoi polygons of a plant and its neighbours can be used in studying aspects of the plant's performance including survival rate, growth rate, size and weight (Kenkel, 1990). Examples of such studies are provided by Hasegawa *et al.* (1981), Liddle *et al.* (1982), Watkinson *et al.* (1983), Bulow-Olsen *et al.* (1984), Mithen *et al.* (1984), Hutchings and Waite (1985), Matlack and Harper (1986), Firbank and Watkinson (1987), Kenkel *et al.* (1989), Owens and Norton (1989), and Zhang and Hamill (1997). In a comparative evaluation of the ability of a wide range of competition measures to predict the growth of loblolly pine trees, Daniels *et al.* (1986) find that the Voronoi polygon approach performs at least as well

as the other measures and is particularly effective when other tree and stand characteristics are known.

Given the assumptions of the Voronoi Assignment Model the most appropriate applications are to monospecific stands of upright plants with simultaneous germination (Mithen *et al.*, 1984) especially in the first few months after germination when individual plant growth rates are most similar, thus ensuring that most plants are of approximately the same size (Matlack and Harper, 1986). When these conditions do not hold, a weighted Voronoi diagram may be appropriate with weights reflecting, for example, differences in tree diameters (Moore *et al.*, 1973; Zuuring *et al.*, 1984; Nance *et al.*, 1987), tree heights (Pelz, 1978), or plant germination times (Kenkel, 1991). Voronoi polygon models can also be used when more than one species of plant occupies the same environment, but since such models involve spatial competition, they are discussed in Section 7.4.

A variant of this use in plant ecology is provided by Hasegawa *et al.* (1981) in their study of the crown projection diagrams of trees in a forest. They propose that if identical trees develop uniformly in a uniform environment the crown projection diagram will be equivalent to a Voronoi diagram. To test this they construct the Voronoi diagram associated with the areal centres of gravity of the crowns of a stand of Japanese cedars (*Cryptomenia japonica*) and compare this with the actual crown projection diagram. A good measure of fit is found between the two diagrams, but some differences do exist because some degree of overlap and small unfilled areas are observed in the actual crown projection diagram which are not present in the Voronoi diagram.

Voronoi Assignment Models are also applicable to animal territories defined with respect to specific point locations such as nests, roosts and food caches (Tanemura and Hasegawa, 1980) while Byers (1992, 1996) uses Voronoi diagrams of points of entry to examine the spatial patterns of attack of different species of bark beetles on conifers.

Social scientists studying various types of territorial structures associated with humans have also made extensive use of Voronoi Assignment Models. Unlike many of their physical counterparts, human spatial patterns rarely show a high degree of regularity, although one celebrated instance occurs in geography in the context of *central place theory* (see King, 1984, for a review). This is concerned with explaining the size and spacing of nucleated settlements (central places) which provide goods and services to rural customers distributed over a geographical region. One aspect of this theory relates to the definition of the trade areas (areas of influence) associated with the central places for a specified good or service. In classical central place theory (Christaller, 1933; Lösch, 1954) the locations of the central places are assumed to form a triangular lattice (see Figure 8.2.2) and the rural population is assumed to be uniformly distributed over the region. In addition, it is assumed that

(i) every central place provides the good or service under consideration;
(ii) consumers travel to a central place to acquire the good or service;

(iii) the market price, m, of the good or service is the same at all central places;
(iv) the cost, c, to the consumer of acquiring the good or service is equal to the market price plus the cost of transportation, t, to the central place ($c = m + t$);
(v) $t = rd$, where d is the Euclidean distance travelled by the consumer and r is the transportation rate per unit distance;
(vi) customers minimize the cost of purchasing the good or service.

Taken collectively assumptions (ii)–(vi) imply that consumers will patronize the nearest central place. Thus, the trade areas are equivalent to the Voronoi polygons of the central places (Dacey, 1965) and in the case of classical central place theory they will be regular hexagons.

These concepts can be extended directly to situations involving any type of settlement spacing. Thus, Bogue (1949) and Snyder (1962) use the Voronoi Assignment Model to define Voronoi polygons around US metropolitan centres and Uruguayan urban centres, respectively, which are considered proxies for the real market areas of these centres. Ohji (1986) used them to define market areas for periodic markets in Kanataka State in southern India.

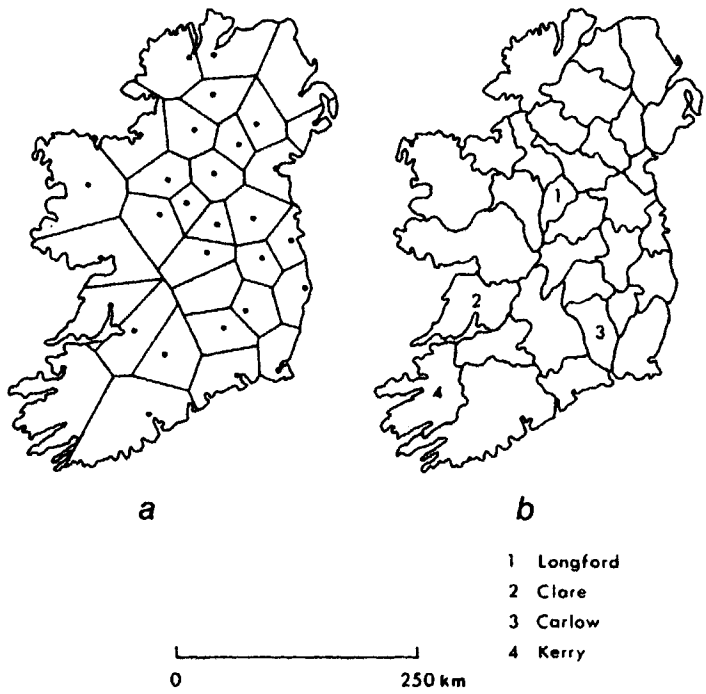

Figure 7.1.9 Counties of Ireland. (a) Theoretical partition created by the Voronoi diagram of county towns. (b) Actual counties. (Redrawn from data in Cox and Agnew, 1976.)

In each case the market areas so created correspond to areas over which the centres exercise a spatial monopoly. Identical concepts have been applied to a different geographic scale to model the trade areas of individual retail stores (West, 1981; Jones and Mock, 1984; West and von Hohenbalken, 1984; von Hohenbalken and West, 1984; Jones and Simmons, 1987). Polygon adjacencies in the Voronoi diagram of the stores can be used to identify which stores can be considered neighbours and thus are likely to be in direct competition.

Such considerations are also relevant in modelling the service areas of facilities providing public services. Suppose that we consider a set of facilities at fixed locations in a region which provide a service to a set of individual users distributed over the same region. The service may either be dispensed to the users at their locations or offered at the facility to which the users must travel. Obvious examples of such facilities are those providing public services such as health and education. If we assume that the facilities are identical, that there are no constraints on the number of people who can use a facility and that, in order to minimize costs of acquiring the service, users are served by the nearest facility, the service areas of the facilities will be equivalent to their Voronoi polygons (Goodchild and Massam, 1969; Keeney, 1972). Note that the last of these assumptions means that the aggregate distance travelled between users and facilities is minimized. This situation is usually referred to as the *unconstrained transportation problem* (Scott, 1971, p. 118; Keeney, 1972; Massam, 1972, pp. 9–10; 1975, pp. 59–60). While such a formulation may be unrealistic in empirical situations since facility constraints almost always occur and that, if allowed to choose, users do not always go to the nearest facility, the Voronoi diagram is often used as a normative structure against which the empirical or other proposed structures are evaluated. Goodchild and Massam (1969) follow such a strategy in evaluating the efficiency of electricity supply service areas in southern Ontario, Canada. Similarly, Cox and Agnew (1976) use the Voronoi diagram of the existing county towns of Ireland to create a theoretical partition (Figure 7.1.9(a)) against which the existing set of counties (Figure 7.1.9(b)) is compared. Using an information-theoretic measure, they determine that there is an overall spatial correspondence of 72% between the two structures. However, the measures of agreement between individual counties is quite variable being highest for large coastal counties such as Clare (92%) and Kerry (90%) and lowest for small inland counties such as Carlow (40%) and Longford (44%). Boyle and Dunn (1991) use Voronoi edges to approximate enumeration districts in England.

The Voronoi assignment model has also been used to determine various kinds of social boundaries. For example, Singh (1976, 1979), Singh and Singh (1975, 1977, 1978) and Callen and Stephan (1975) use the edges of the Voronoi diagram of village sites in the Middle Ghanga Valley in India and Bougainville Island in the Solomons, respectively, to simulate village boundaries. However, the most extensive work of this kind involves the identification of linguistic boundaries (isoglosses) and follows an approach

developed by Haag (1898) in a study of dialects in south-west Germany. He begins by generating the Voronoi diagram of a set of localities at which dialect data have been recorded. An edge of the Voronoi diagram is then 'decorated' if the two localities sharing the edge differ in terms of a dialect feature (e.g. the pronunciation of a particular word). In this way, highly decorated edges represent important linguistic divides and the resulting map is sometimes referred to as a *Kombinationskarte*. While the general idea of producing such a map (later called a *Wabenkarte* or *honeycomb*) became adopted widely, Haag's method of using the Voronoi diagram to determine the geographical location of the edges did not (see Handler and Wiegand, 1982, for review of the subsequent development of this approach). However, with the widespread availability of computer software for constructing the Voronoi diagram, Haag's method has experienced a resurgence in popularity (Goebl, 1981, 1983, 1987, 1993; Schlitz, 1996). Linguistic differences between neighbouring dialect data sites can also be represented by values attached to the edges of the Delaunay tessellation of these sites (Goebl, 1983). Oden *et al.* (1993) developed a procedure (categorical wombling) which uses several graph-theoretic statistics to determine if Delaunay edges linking dissimilar sites can be significantly configured into boundaries or if they tend to significantly enclose regions of homogeneous linguistic characteristics. Fortin (1994) has also employed this strategy to identify transition zones (ecotones) between adjacent communities in ecological data.

In archaeology, the Voronoi Assignment Model has been used to identify possible territorial structures of early civilizations by defining Voronoi polygons around significant sites. Examples include Iron Age (first century BC) southern England (Cunliffe, 1971; Lock and Harris, 1996), Minoan Crete (Renfrew, 1972), the Maya lowlands (Hammond, 1972, 1974), Roman Britain (Hodder, 1972), Malta (Renfrew, 1973b), Neolithic Wessex, England (Renfrew, 1973a), Mycenaean Greece and Etruria (Renfrew, 1975), the Late Archaic in the Savannah River valley of Georgia and South Carolina (Savage, 1990) and Aztec sites in the Basin of Mexico (Ruggles and Church, 1996). However, if the sites differ significantly, as would occur, for example, if they were part of a hierarchically organized social system, generalized Voronoi diagrams are more appropriate (see Section 3.1.6 for examples of such work).

The final application of the Voronoi Assignment Model to be discussed arises in the study of codes. In very general terms, coding involves the translation of a signal from one form to another (Agrell, 1997, p. v). In vector quantization the input signal has the form of a real valued vector $\boldsymbol{x}$ in m-dimensional Euclidean space $\mathbb{R}^m$ and encoding involves examining a code book C, consisting of a finite set of codevectors $\boldsymbol{c}_i$, to identify the codevector which best represents $\boldsymbol{x}$ (Agrell and Hedelin, 1994). This can be done by identifying the codevector which is geometrically closest to $\boldsymbol{x}$, i.e. the one whose Voronoi region contains $\boldsymbol{x}$. Since this procedure was labelled minimum distance or maximum likelihood coding (Shannon, 1959), when used in this context the Voronoi regions were originally referred to as *maximum likelihood regions* (Slepian, 1965, 1968). Essentially the same problem occurs in

decoding when a receiving device must search a set of possible transmitted signals to determine the one which underlies the observed signal (Landau, 1971). The most frequently used measure of the error resulting from quantization, the mean squared error, or distortion D, per vector can be expressed in terms of Voronoi regions (Agrell and Eriksson, 1998) as

$$D = \sum_{i=1}^{N} \int_{V(\boldsymbol{c}_i)} \|\boldsymbol{x} - \boldsymbol{c}_i\| f_{\boldsymbol{x}} \, \mathrm{d}\boldsymbol{x}, \tag{7.1.7}$$

where N is the number of codewords; $V(\boldsymbol{c}_i)$ is the Voronoi region of $\boldsymbol{c}_i$; and $f_{\boldsymbol{x}} \, \mathrm{d}\boldsymbol{x}$ is the probability density function of the input vectors $\boldsymbol{x}$.

A well-known conjecture in quantization theory (Gersho, 1979) states that when the number of codevectors is sufficiently large, the optimal vector quantizer for a uniformly distributed $\boldsymbol{x}$ will consist of Voronoi regions almost all of which (the exceptions are due to edge effects) are congruent to some polytope H. Consequently, attention has focused on structured codes whose Voronoi regions possess this quality. Such codes include those based on modified lattices (Agrell and Eriksson, 1998; Baranovskii, 1991; Conway and Sloane, 1982, 1983, 1984, 1991, 1992, 1993; Eriksson and Agrell, 1996; Gersho, 1979, 1982; Moody and Patera, 1995; Viterbo and Biglieri, 1996; Worley, 1987, 1988) and block codes (Agrell, 1996, 1997; Shannon, 1959). Note that when a lattice is used as a vector quantizer for uniformly distributed input vectors, D in equation (7.1.7) is equal to the normalized second moment of inertia of the Voronoi cell of the lattice.

A (m, k) binary linear block code consists of 2^k codewords each of which is a block of m bits. When the values 0 and 1 are considered as coordinates, the codewords lie on the vertices of a hypercube, whose centre $(1/2, \ldots, 1/2)$ is the one and only vertex of all Voronoi regions (i.e. the Voronoi regions are conical). In this case, all regions are the same shape and those that are Voronoi neighbours are also Gabriel (full) neighbours (Agrell, 1996, 1997). Binary linear block codes are part of a larger class of codes known as group codes (Slepian, 1965, 1968) which in turn are included in the class of geometrically uniform codes (Forney, 1991). This group also includes lattice-based codes and spherical codes (Gao *et al.*, 1988). General properties of the Voronoi regions of group codes and geometrically uniform codes are given by Slepian (1968) and Forney (1991), respectively.

The use of the Voronoi Assignment Model to address problems in coding can also be extended to conceptually similar situations such as re-sampling in remote sensing when values from spatially irregularly sampled sites must be converted to values at grid sites (Gotsman and Lindenbaum, 1995).

7.2 GROWTH MODELS

These models produce spatial patterns as the result of a simple growth process operating with respect to a set of n points (nucleation sites), $P = \{p_1, p_2, \ldots, p_n\}$, at positions $\boldsymbol{x}_1, \boldsymbol{x}_2, \ldots, \boldsymbol{x}_n$, respectively, in $\mathbb{R}^m$ or a bounded

region of $\mathbb{R}^m$ ($m = 2, 3$). If we make the following assumptions, the resulting pattern will be equivalent to the ordinary Voronoi diagram, $\mathcal{V}(P)$, of P:

Assumption VGM1 Each point p_i ($i = 1, 2, \ldots, n$) is located simultaneously.

Assumption VGM2 Each point p_i remains fixed at x_i throughout the growth process.

Assumption VGM3 Once p_i is established, growth commences immediately and at the same rate, l_i, in all directions from p_i.

Assumption VGM4 l_i is the same for all members of P.

Assumption VGM5 Growth ceases whenever and wherever the region growing from p_i comes into contact with that growing from p_j ($j \neq i$).

Collectively, assumptions VGM1–VGM5 define the *Voronoi Growth Model.* Figure 7.2.1 shows a series of stages in such a growth process.

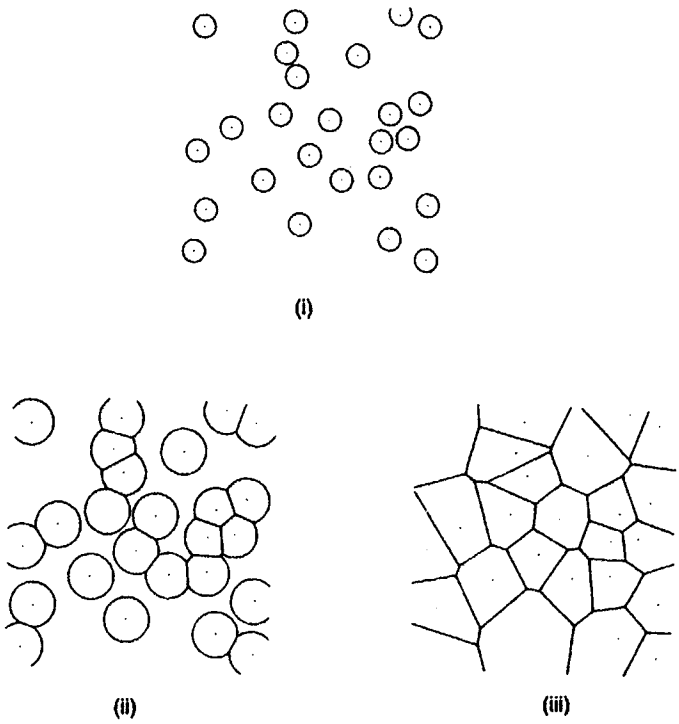

Figure 7.2.1 Stages (i), (ii) and (iii) of the Voronoi growth model.

Although the Voronoi Growth Model has been applied in a variety of different circumstances, the range of applications is not as great as that for the Voronoi Assignment Model and most are found in the natural sciences. One obvious application is to model crystal growth about a set of nucleation sites (Avrami, 1939; Leonyuk and Mal'tseva, 1980). Here Assumptions VGM3–VGM5 are equivalent to assuming an omnidirectional, uniform supply of crystallizing material to all faces of the growing crystal in the absence of any adsorbable impurities. Assumption VGM3 also implies that the rate of growth of the volume of a crystal will be proportional to its surface area. Steyer *et al.* (1990) suggest that in two dimensions a close analogy can be made between such crystallization and the growth of droplet condensation patterns, and so they use the Voronoi diagram to model the structure of the patterns of droplets that form when water condenses on the surface of paraffin oil, a liquid in which it is not soluble.

However, probably the most extensive use of growth models is in metallurgy. Here a major use is in modelling phase transitions involving the transformation of an isotropic, one-component solid through nucleation, and the isotropic growth of grains of a new or re-crystallized phase (Watson and Smith, 1975; Mahin *et al.*, 1980; Burger *et al.*, 1988; Vaz and Fortes, 1988; Marthinsen *et al.*, 1989). In this context the Voronoi Growth Model is sometimes referred to as the *cell model* (Meijering, 1953) or the *site saturation model* (Saetre *et al.*, 1986). Specific examples include covering a metallic surface with films or layers of a corrosive product (Evans, 1945) where the nucleation sites, P, might be surface imperfections such as impurities, points of intersection with bulk defects and surface pits (Frost and Thompson, 1987a). Another example is the growth of thin films of metal or semiconductors (Frost and Thompson, 1988). In these examples, if the thickness of the film is small relative to the spacing between the nucleation sites or if the grain boundaries are perpendicular to the plane of the film, a two-dimensional representation is appropriate.

An interesting application of the Voronoi Growth Model occurs in astronomy, where it has been used to describe the morphology of the large-scale structure of the universe. In one set of models (Matsuda and Shima, 1984; Icke and van der Weygaert, 1987, 1991; Coles and Barrow, 1990; Webster, 1998) it is suggested that a collection of slightly underdense regions in a primordial density field will act as the seeds of voids or expansion centres ('superhubble bubbles') from which matter will flow outwards until it encounters similar material flowing from another void. If the voids are created simultaneously, and the excess expansion is the same for all voids, we have the equivalent assumptions to those specified above for the Voronoi Growth Model. Once defined, the Voronoi diagram associated with the voids forms a skeleton around which the galaxies assemble during the evolution of the universe. In $\mathbb{R}^3$ the faces of the Voronoi polyhedra can be interpreted as the contact surfaces ('Pancakes'), their edges as elongated 'superclusters' and their nodes as virialized 'Abel clusters'. Van de Weygaert and Icke (1989) propose that the density at the facets of the Voronoi polyhedra of material

diffused from the voids is inversely proportional to the dimensionality of those facets so that over time galaxies tend to congregate at the highest density locations (the Abel clusters).

Another model, proposed by Yoshioka and Ikeuchi (1989), involves seed objects which explode simultaneously and with the same energy, thus forming shockwaves which expand into the intergalactic medium. The expanding shockwaves carry with them any mass particles which they encounter, thus concentrating the mass particles on the two-dimensional surfaces where the expanding shockwaves come into neutral contact. The result is again a Voronoi diagram in $\mathbb{R}^3$.

A variety of different point processes (see Section 5.12) has been used to model the locations of the seeds of both the gravitational instability and explosion models including the homogeneous Poisson (Yoshioka and Ikeuchi, 1989; Coles, 1990; Ikeuchi and Turner, 1991; van de Weygaert, 1991, 1994; Zaninetti, 1990, 1992; Goldwirth *et al.*, 1995; Doroshkevich *et al.*, 1997), hard core (van de Weygaert, 1994; Ryden, 1995), Poisson cluster (van de Weygaert, 1994), displaced lattice (SubbaRao and Szalay, 1992), fractal (Martinez *et al.*, 1990; Zaninetti, 1991b, 1993), Sobol (Zaninetti, 1992) and the eigenvalues of random complex matrices (Zaninetti, 1992). The models have also been extended to consider other types of Voronoi diagram including the additively weighted (Johnson–Mehl) (Icke and van de Weygaert, 1991) with either random or Gaussian points (Zaninetti, 1991a; Molchanov *et al.*, 1997), and line (representing strings of seeds) (Zaninetti, 1991b).

The Poisson Voronoi diagram in $\mathbb{R}^3$ has also been used as the basis of a model to explore other astronomical phenomena where the overall structure has a basic cellular topology (Pierre, 1990) such as Lyman Alpha absorbers at high redshifts (Pierre *et al.*, 1988).

The Voronoi Growth Model has also been used in geology in several circumstances. One is in modelling crack patterns in general and cracking in basalt (lava flows), in particular, where the crack patterns result from the contraction of the material on cooling. An early application is provided by Stiny (1929) who proposed that, as a molten stream of basalt cools irregularly at its surface, the locations where hardening occurs first act as nuclei from which subsequent cooling extends in all directions throughout the material. Thus, tensile stress can be modelled as a set of expanding circles centred at the nuclei which, as they meet, develop lines along which cracking occurs. Smalley (1966) seems to have developed a similar model independently. He argues that if the basaltic material is of uniform temperature, the nuclei will appear simultaneously and form a regular spatial arrangement in the form of a triangular lattice (see Figure 8.2.2) so that growth centred on them produces hexagonal blocks of basalt. However, if uniformity of temperature does not occur, as is usually the case, the nuclei will not develop simultaneously and will not form a regular arrangement. Smalley (1966) suggests that in such circumstances the growth process should be applied to centres located according to a hard core process of the type described in Section 5.12, whereby centres are located at random subject to the constraint that centres

that are closer than some specified distance to an already existing centre cannot develop. He ran a number of simulations of this model and examined the frequency distribution of N, the number of neighbours (edges, vertices) of an individual Voronoi polygon (block of basalt). These frequencies were compared with those obtained from real world basalt patterns and found to differ in a statistically significant way. Smalley argues that such discrepancies could arise due to the difficulty of identifying very short edges in field counts of N. Thus, he ignored such small edges in his simulated patterns before recalculating the frequencies of N associated with them. These modified model frequencies provide a better fit to the empirical data than the original model frequencies but again the differences between the two sets are statistically significant. Further evidence for questioning the validity of the Stiny/Smalley model is provided by Stoyan and Stoyan (1980) who demonstrate that at least one empirical pattern of basalt blocks does not strongly approximate a Voronoi diagram.

Also in geology, Williams (1972, p. 152) has proposed that the Voronoi Growth Model is appropriate for modelling the polygonal depressions that develop in karst topography. Here the nuclei around which growth develops are stream sinkholes.

Ecological applications of the Voronoi Growth Model occur in the study of plant and animal territories where the Voronoi diagram defined with respect to a set of individuals, each with an associated fixed location in $\mathbb{R}^2$, can be considered to represent ideal territories if the environment is ecologically uniform and the plants are even-aged and genotypically homogeneous (Galitsky, 1990) or the animals are of equal strength (Hasegawa and Tanemura, 1976; Gibson and Ashby, 1988). An example is provided by the territories of male mouthbreeder fishes (*Tilapa mossambica*) observed by Barlow (1974). These fish were kept in an outdoor pool with an initially uniform sandy bottom. The males excavate breeding pits by spitting sand away from fixed pit centres towards the pit centres of their neighbours. Reciprocal spitting results in sand parapets which act as territorial boundaries. Figure 7.2.2 shows such boundaries traced by Hasegawa and Tanemura (1976) from a photograph taken by Barlow (1974). Honda (1978) and Suzuki and Iri (1986a) (see Section 9.5.2) show that the pattern of such boundaries closely approximates the edges in the Voronoi diagram with the breeding pits as generators (see Figure 9.5.2).

Unlike the Voronoi Assignment Model, there have been far fewer applications of the Voronoi Growth Model to phenomena studied by social scientists. One example is provided by Boots (1973, 1975a) who used it to investigate patterns of service areas for bus companies as identified by Green (1955). In Britain bus services have their origins in the first few decades of the twentieth century when they first challenged the hegemony of the railways as the prime form of longer distance public transportation. The development of these services was not coordinated by any central agency and the process was a highly competitive one. Bus services tended to become established at the urban centres which already provided surrounding rural

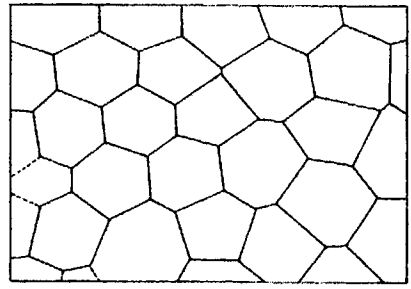

Figure 7.2.2 Schematic diagram of polygonal territories formed by male mouthbreeder fish replicated from a photograph in Barlow (1974). (*Source*: Hasegawa and Tanemura, 1976, Figure 1.)

areas with other goods and services. In areas away from the major urban agglomerations, such centres are relatively similar in size and so if the bus services were established at these places at approximately the same time, the Voronoi Growth Model could describe the service areas that arose under competition between centres. Although no formal statistical tests were undertaken, summary statistics for the characteristics of the bus service areas, such as number of neighbours, area and boundary length, were found to be similar to those expected for Voronoi polygons.

It is important to note that both the Voronoi Assignment and Growth Models can be modified to produce a whole set of extended models by changing one or more of their underlying assumptions. For instance, by changing Assumption VAM1 or VGM1 the points can be introduced into $\mathbb{R}^m$ asynchronously, giving rise to Johnson–Mehl type models such as those described in Section 5.8. Changing Assumption VAM2 or VGM2 produces dynamic models of the type discussed in Section 7.5. Assumption VAM3 can be modified to consider unequal points by assigning to each point a weight which reflects its relative importance. Such differential weights might also be reflected in differences in the growth rates associated with individual points in the Voronoi Growth Model, thus revising Assumption VGM4. The weights could also be used in defining how the distance between a member of P and other locations in $\mathbb{R}^m$ is measured, thus leading to assignment procedures which differ from those in Assumption VAM4. Such models and their applications are discussed in Chapter 3. Assumption VGM4 can also be modified to allow for growth to vary with direction from p_i. For instance, in the anisotropic Voronoi diagram proposed by Scheike (1994) (see Section 3.7.2), cells grow as ellipsoids, all with the same direction. Assumption VGM5 can be changed to allow for growth to terminate before the growing regions fill the space (e.g. before stage (iii) in Figure 7.2.1 is reached). Muche (1993) labels the resulting structure an incomplete Voronoi diagram (see Section 5.6.2). This structure has been extensively studied for the situation in which the points are located according to a homogeneous Poisson point process (see Section 1.3.3) in two dimensions (Schulze and Schwan, 1992, 1993; Schulze *et al.* 1989, 1993; Schulze and Wilbert, 1989b).

Finally, we note that while this section has described how the Voronoi Growth Model has been used to model physical systems, Tolmachiev and

Adamatzky (1996) propose a reversal of roles and suggest that an appropriate physical process can be used as an alternative way of computing a Voronoi diagram. First, they create a chemically active substrate by spreading a thin film of agar gel mixed with palladium chloride ($PdCl_2$) on a clear acetate film. Drops of potassium iodide liquid (KI) are then applied at sites corresponding to the Voronoi generator points. As the KI liquid diffuses over the film, it reacts with the $PdCl_2$ to produce PdI_2 as a precipitate, thus colouring the film black. However, at locations where waves of KI diffusing from different sites meet, the concentration of $PdCl_2$ is insufficient to be involved in the reaction. As a result, the interiors of the Voronoi cells appear black while their edges remain uncoloured (white). Antecedents of such chemical processors are found in the 'hardware models' of Morgan (1967). A simple model of his uses only ordinary pink blotting paper and a solvent of *N*-butanol. The solvent is supplied to the blotting paper by means of small wicks located at the generator points of the Voronoi diagram. As the solvent spreads out from each of the wicks, it carries with it some of the red pigment in the blotting paper, so that when the process is finished and the paper is dried, the limits of the solvent front are marked by thin red lines which represent the edges of the Voronoi diagram. For the specific case of the Poisson Voronoi diagram (see Chapter 5), Schulze and Schulze (1992) and Schulze and Wilbert (1989a, 1991a,b) show how this may be realized experimentally by heat treatment of polypropylene foil.

7.3 SPATIAL–TEMPORAL PROCESSES

In the preceding sections we dealt with spatial processes leading to Voronoi diagrams in which the locations of generators do not change over time. In this section we show some models of spatial processes in which the location of generators change over time.

7.3.1 Spatial competition models: the Hotelling process

In economics, in particular in spatial economics (or urban economics), a considerable number of studies have been carried out to examine market area stability (a review is provided, for example, by Gabszewicz *et al.*, 1986). Economic units, say firms, compete with each other to maximize their profits. In a spatial context, this competition takes the form of market area competition. If consumers buy products from the firm that offers the lowest price, each firm has its own market area. The market areas are different in size, yielding different profits, and firms with small profits move to alternative locations to gain more profits. Through this relocation process the configuration of firms may vary over time, or it may eventually reach an equilibrium configuration. The pioneering work on this market area stability was done by Hotelling (1929). A variety of models have been developed from his model, which we call Hotelling processes or, more broadly, spatial

competition processes. In this subsection we investigate spatial competition processes with the simplest Hotelling model, i.e. the Alonso version (Alonso, 1964) of the original Hotelling (1929) model.

Suppose that there are n firms located at $x_1, \ldots, x_n$ in a region S, and these firms are selling the same products with the same mill price (the price not including a delivery cost). We assume that the delivery cost from a firm at x_i to a consumer at x is proportional to the Euclidean distance $\|x_i - x\|$, and that consumers buy the products from the firm that quotes the lowest delivered price (the mill price plus the delivery cost). Under these assumptions, the configuration of n market areas is represented by the ordinary Voronoi diagram $\mathcal{V}(P) = \{V(x_1), \ldots, V(x_n)\}$, and the market area of firm i is represented by the Voronoi polygon $V(x_i)$. We further assume that the demand for the products is uniformly distributed over the region S; the marginal cost of the products is the same for all firms; and the relocation cost is negligibly small. Then the profit of firm i is proportional to the area of $V(x_i)$. The firms compete in terms of their locations to maximize their profits. As a result, we observe a spatial competition process of n firms over time. We specify this process by the following behavioural assumptions.

Assumption HP1 (relocation timing) Each firm considers relocation once in every period, and the interval is equal over time periods.

Assumption HP2 (zero conjectural variation) In considering possible relocation, every firm conjectures that each firm will not change its location.

Let $X_{-i} = \{x_1, \ldots, x_{i-1}, x_{i+1}, \ldots, x_n\}$ be the set of locations of all firms except firm i, and x_i^* be the location of firm i that yields the maximum profit provided that the locations of the other firms are fixed at the present locations, i.e.

$$|V(x_i^*)| = \max_{x \in S} \left\{ |V(x)| \mid X_{-i} \text{ is fixed}, x \neq x_j, j \in I_n \backslash \{i\} \right\}, \tag{7.3.1}$$

where $|V(x)|$ indicates the area of $V(x)$. As is indicated by the condition in equation (7.3.1), firm i is not allowed to locate at the same location as any other firms.

We add one more behavioural assumption.

Assumption HP3 (relocation decision) Firm i moves to the location x_i^* (given by equation (7.3.1)) if the location x_i^* yields a greater profit than the present profit, i.e. $|V(x_i^*)| > |V(x_i)|$. Otherwise, firm i remains at the present location x_i.

We call the process characterized by the above assumptions the *Hotelling process*. Stated abstractly, the Hotelling process is the process in which each generator independently moves to maximize the area of its Voronoi polygon. Through the Hotelling process, the Voronoi diagram may change over time,

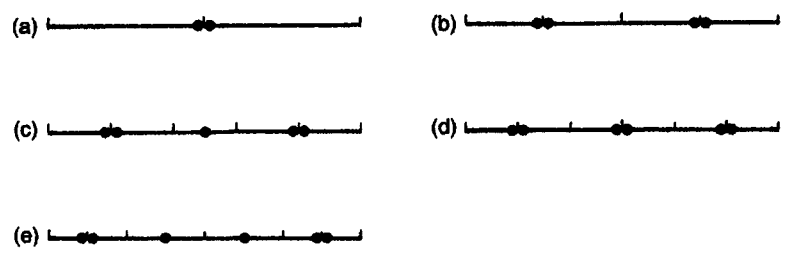

Figure 7.3.1 Global equilibrium configurations (Voronoi diagrams) of n firms on a bounded line market ($n = 2, 4, 5, 6$).

or it may eventually reach an equilibrium state in which all firms have no incentive to relocate. To be precise, the configuration of the n firms is in *global equilibrium* if and only if no firm can find a more profitable location than the present location; that is, the Voronoi diagram $\mathcal{V}^* = \{V(x_1^*), \ldots, V(x_n^*)\}$ is in *global equilibrium* if and only if

$$|V(x_i^*)| > \max_{x_i \in S} \{|V(x_i)| \mid X_{-i} = X_{-i}^*,\ x_i \neq x_j^*, j \in I_n \backslash [i]\} \qquad (7.3.2)$$

$$\text{for any } i \in I_n,$$

where $X_{-i}^* = \{x_1^*, \ldots, x_{i-1}, x_{i+1}, \ldots, x_n^*\}$.

When S is a bounded one-dimensional space, we can obtain the exact global equilibrium configurations $\mathcal{V}^*$ (Eaton and Lipsey, 1975a), which are shown in Figure 7.3.1. For $n = 2$, 4 and 5, we have the unique global equilibrium configuration; for $n = 3$, we have no global equilibrium; for $n \geq 6$, we have an infinite number of equilibrium configurations. Two extreme configurations are shown in panels (d) and (e).

The Hotelling process in a two-dimensional space was first studied by Eaton and Lipsey (1975a, b), followed by Shaked (1975), Okabe and Suzuki (1987), Okabe and Aoyagi (1991) and Aoyagi and Okabe (1993). Compared with the one-dimensional space, analytical examination becomes very difficult owing to complicated geometric calculations. We first show a few basic properties about the variation of the area of a Voronoi polygon. These properties are useful not only for the following analysis but also for locational optimization to be discussed in Chapter 9.

Consider a Voronoi diagram $\mathcal{V} = \{V(\boldsymbol{x}), V(\boldsymbol{x}_1), \ldots, V(\boldsymbol{x}_{n-1})\}$, where $\boldsymbol{x}^{\mathrm{T}} = (x, y)$ is the location of firm 0, and suppose that firms $1, \ldots, m$ share their market boundaries with firm 0 (firms $1, \ldots, m$ are indexed counterclockwise around firm 0). Let $\boldsymbol{u}_i^{\mathrm{T}} = (u_i, v_i)$ be the Cartesian coordinates of the Voronoi vertex shared by $V(\boldsymbol{x})$, $V(\boldsymbol{x}_i)$ and $V(\boldsymbol{x}_{i+1})$. Recalling that a Voronoi vertex is the intersection of two bisectors (Chapter 2), we can write (u_i, v_i) in terms of $\boldsymbol{x}$, $\boldsymbol{x}_i$ and $\boldsymbol{x}_{i+1}$, from which we can obtain the area of a Voronoi polygon $V(\boldsymbol{x})$. Since this quantity is frequently used in many applications, we state it as a formula.

The area of a Voronoi polygon

$$|V(\boldsymbol{x})| = \frac{1}{2}\sum_{i=1}^{m}\left(u_i(x,y)v_{i+1}(x,y) - u_{i+1}(x,y)v_i(x,y)\right), \tag{7.3.3}$$

where

$$\begin{aligned} u_i(x,y) &= \frac{(x_i^2+y_i^2-x^2-y^2)(y-y_{i+1}) - (x_{i+1}^2+y_{i+1}^2-x^2-y^2)(y-y_i)}{2\{(x_i-x)(y_{i+1}-y)-(x_{i+1}-x)(y_i-y)\}}, \\ v_i(x,y) &= \frac{(x_i^2+y_i^2-x^2-y^2)(x-x_{i+1}) - (x_{i+1}^2+y_{i+1}^2-x^2-y^2)(x-x_i)}{2\{(x_i-x)(y_{i+1}-y)-(x_{i+1}-x)(y_i-y)\}}, \end{aligned} \tag{7.3.4}$$

where $u_{m+1} = u_1$, $v_{m+1} = v_1$, $x_{m+1} = x_1$ and $y_{m+1} = y_1$.

From equations (7.3.3) and (7.3.4) we readily notice that $|V(\boldsymbol{x})|$ is continuous except at $\boldsymbol{x} = \boldsymbol{x}_i$ unless m changes. We should next examine whether or not $|V(\boldsymbol{x})|$ is continuous even if m changes (this question is closely related to a more general problem, called the *moving generator (particle) problem*; Cruz Orive, 1979). To consider this question, we depict Figure 7.3.2 where the filled circles show the fixed generators and the unfilled circle indicates the initial location, o, of the moving generator $\boldsymbol{x}$. The initial shape of $V(\boldsymbol{x})$ at $\boldsymbol{x} = \boldsymbol{0}$ is a hexagon (the heavy broken lines in Figure 7.3.2). Suppose that the generator $\boldsymbol{x}$ moves along a line radiating from o, indicated by the dash-dot line in Figure 7.3.2. When the generator $\boldsymbol{x}$ comes to the point indicated by the unfilled square, $V(\boldsymbol{x})$ becomes a septagon (the dotted lines in Figure 7.3.2). There must be a point between the unfilled circle and the unfilled square on the dash-dot line at which the shape of $V(\boldsymbol{x})$ changes from a hexagon to a septagon. The following property gives the answer to this question.

Property HP1 Consider a Voronoi diagram $\mathcal{V} = \{V(\boldsymbol{x}), V(\boldsymbol{x}_1), \ldots, V(\boldsymbol{x}_{n-1})\}$, where $V(\boldsymbol{x})$ is adjacent to $V(\boldsymbol{x}_1), \ldots, V(\boldsymbol{x}_m)$ when $\boldsymbol{x} = \boldsymbol{0}$. Suppose that as the generator $\boldsymbol{x}$ moves from $\boldsymbol{0}$ along a line L radiating from $\boldsymbol{0}$, a Voronoi vertex $\boldsymbol{u}_{m+1}$ appears between vertices $\boldsymbol{u}_i$ and $\boldsymbol{u}_{i+1}$ (or $\boldsymbol{u}_i$ and $\boldsymbol{u}_{i+1}$ degenerate into one vertex $\boldsymbol{u}_m$). Let C be the circle that passes through points $\boldsymbol{x}_i, \boldsymbol{x}_{i+1}$ and $\boldsymbol{x}_m$, and $\boldsymbol{x}^*$ be a point at which the line L meets the circle C. Then $\boldsymbol{x}^*$ is the point at which $V(\boldsymbol{x})$ changes from an m-gon to an $(m+1)$-gon (or $(m-1)$-gon).

We can prove this property from the empty circle property (Property D5) in Chapter 2. The detailed derivation is shown by Cruz Orive (1979) for special lattice configurations and by Okabe and Aoyagi (1991) for general configurations.

Using Property HP1, we can determine regions for $\boldsymbol{x}$ in which $V(\boldsymbol{x})$ is an m-gon for a given configuration of generators. An example is shown in Figure 7.3.2, where generators are placed on regular triangular lattice points. (Note that generators are not necessarily spaced regularly.) The number in each region enclosed by circular arcs indicates m of $V(\boldsymbol{x})$.

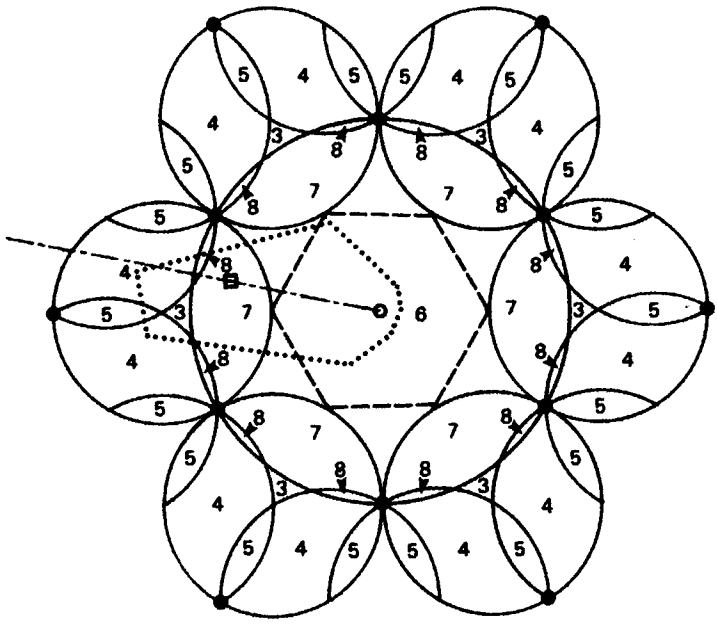

Figure 7.3.2 The shape of a Voronoi polygon $V(\boldsymbol{x})$ whose generator $\boldsymbol{x}$ moves on the plane where the other generators are fixed at regular triangular lattice points (the number m in each region enclosed by circular arcs indicates the number of vertices of $V(\boldsymbol{x})$ when $\boldsymbol{x}$ comes to that region).

From equations (7.3.3) and (7.3.4) with Property HP1, we can show, after a few steps of derivation, that $|V(\boldsymbol{x})|$ is continuous with respect to $\boldsymbol{x}$ $(\neq \boldsymbol{x}_i)$ not only when m does not change but also when m changes. In addition, we can show the following property.

Property HP2 For fixed $\boldsymbol{x}_1, \ldots, \boldsymbol{x}_{n-1}$ and $\boldsymbol{x} \neq \boldsymbol{x}_i \in I_{n-1}$

(i) $|V(\boldsymbol{x})|$ is continuous with respect to $\boldsymbol{x}$;
(ii) $\partial |V(\boldsymbol{x})| / \partial \boldsymbol{x}$ exists and it is continuous with respect to $\boldsymbol{x}$.

It is straightfoward to obtain the first derivative of equation (7.3.3), from which we can easily notice that the derivative is continuous with respect to $\boldsymbol{x}$ unless m changes. If m changes, we can prove the continuity of the first derivatives using Property HP1. The detailed derivation is shown in Okabe and Aoyagi (1991). Note that the second derivatives are not necessarily continuous.

It follows from Property HP2 that a necessary condition for the global equilibrium in the Hotelling process is given by

$$\frac{\partial |V(\boldsymbol{x}_i)|}{\partial x_{i\kappa}} = 0, \quad \kappa = 1,2 \text{ for } i = 1, \ldots, n. \tag{7.3.5}$$

When this equation holds, we say that the configuration (Voronoi diagram) of the n firms is in *local equilibrium*.

When the region S is unbounded and firms are located on regular lattice points, it is left as an exercise to examine if the configuration of the firms is in local equilibrium. Using equations (7.3.3)–(7.3.5), we can show that the Voronoi diagram of regular triangular lattice points (Voronoi polygons are hexagons) and that of squares (Voronoi polygons are squares) are in local equilibrium, but the Voronoi diagram of regular hexagonal lattice points (Voronoi polygons are regular triangles) is not in local equilibrium. Furthermore, we can show a stronger property than this property.

Property HP3 The Voronoi diagram of regular triangular lattice points and that of square lattice points are in global equilibrium. The Voronoi diagram of regular hexagonal points is not in local equilibrium; consequently, it is not in global equilibrium.

We can prove this property by computing the Hessian matrix, which is too lengthy to show here (see Okabe and Aoyagi, 1991, in which REDUCE III (algebraic computation software) is used).

When the region S is bounded, analysis becomes extremely intractable except for $n = 2, 3$. Shaked (1975) shows the following property.

Property HP4 When region S is a disc, two firms paired at the centre of the disc are in global equilibrium; there is no local equilibrium for three firms.

See Shaked (1975) for the proof.

The analytical difficulty encountered in a bounded two-dimensional space with $n \geq 4$ firms results from the fact that the optimization problem of equation (7.3.1) is a non-linear, non-convex programming problem. As is shown in the brief review of the non-linear, non-convex programming problem in Chapter 9, it is almost impossible to obtain the global maximum by an analytical method; only a local maximum is obtainable by numerical methods. This intractability prevents analytical examination of the Hotelling process over time, not only in a bounded two-dimensional space but also in an unbounded two-dimensional space. At present it is difficult to say if firms on an unbounded two-dimensional space reach the global equilibrium configurations stated in Property HP3 for any initial configuration. Giving up analytical examination, Eaton and Lipsey (1975b) employed a naive numerical method to examine the Hotelling process for 17 firms in a disc. They conjectured from their numerical results that the global equilibrium configuration would not be achieved. Alternatively, Okabe and Suzuki (1987) imposed the following weaker assumption than Assumption HP3 and examined the Hotelling process over time with numerical simulations.

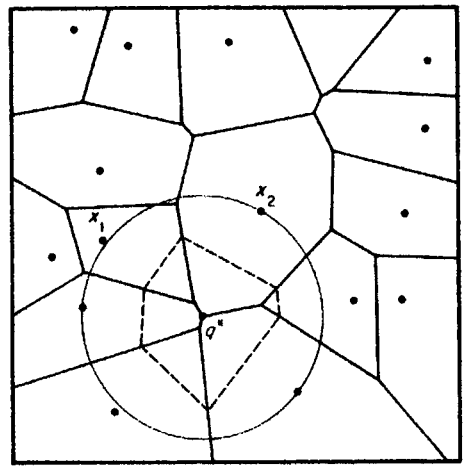

Figure 7.3.3 Searches for local maximum locations $|V(x_1)| < |V(q^*)|$ and $|V(x_2)| > |V(q^*)|$.

Assumption HP4 Let q^* be the centre of the largest empty circle in the Voronoi diagram $\mathcal{V} = \{V(x_1), \ldots, V(x_n)\}$.

(i) If $|V(x_i)| < |V(q^*)|$, firm i searches for a local maximum location x_i^* from q^* (for example, q^* in Figure 7.3.3). If $|V(x_i^*)| > |V(q^*)|$, firm i moves to x_i^*; otherwise firm i moves to q^*.

(ii) If $|V(x_i)| \geq |V(q^*)|$, firm i searches a local maximum location x_i^{**} from the present location (for example, x_2 in Figure 7.3.3). If $|V(x_i^{**})| > |V(x_i)|$, firm i moves to x_i^{**}; otherwise firm i remains at the present location x_i.

Under Assumptions HP1, HP2 and HP4 with the steepest descent method (see Chapter 9), Okabe and Suzuki (1987) carried out the numerical simulation for 256 firms in a square over 100 periods (one period is defined by a period during which every firm makes the locational decision once). Part of the process is shown in Figure 7.3.4, where the filled circles, squares, triangles and stars indicate the change in profit (i.e. a market area) being less than 1%, 1–3%, 3–5%, and more than 5%, respectively. From these numerical results, they notice that although the configuration does not achieve the global equilibrium by the 100th period (observe peripheral firms in Figure 7.3.4), the configuration of inner firms is stable after a certain period of time.

From the simulation of $n = 17$ in Eaton and Lipsey (1975b) and that of $n = 256$ in Okabe and Suzuki (1987), we notice that the stability of the Hotelling process depends upon the number of firms. Moreover, the shape of region S crucially affects the stability. These effects are investigated by Aoyagi and Okabe (1993) theoretically as well as numerically.

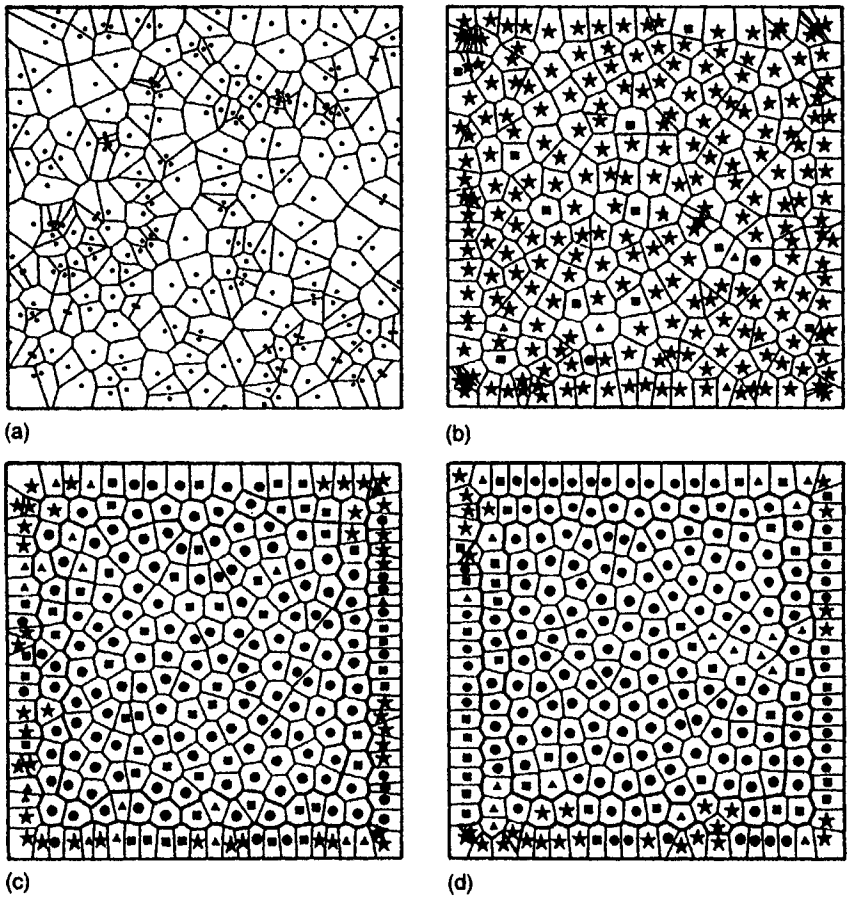

Figure 7.3.4 The Hotelling process of 256 firms in a square region: (a) the initial configuration (uniformly random); (b) the first period; (c) the tenth period; (d) the hundredth period. (The filled circles, squares, triangles and stars indicate the change in profit (i.e. a market area) being less than 1%, 1–3%, 3–5%, and more than 5%, respectively.) (*Source*: Okabe and Suzuki, 1987, Figure 5.)

7.3.2 Adjustment models

Spatial–temporal processes are investigated not only in economic behaviour as we discussed above, but also in animal behaviour. One well-known process is the adjustment process (Hasegawa and Tanemura, 1976). Consider individual animals settled down in a region. In the initial stage, the individuals are fairly independent. As time goes by, however, the individuals interact with each other and each individual tends to occupy its territory in such a way that the individual is as distant from its neighbours as possible. Through this interaction process the territories of the individuals are mutually adjusted until a stable configuration is achieved.

To formulate this process mathematically, let $\boldsymbol{x}_1^{(t)}, \ldots, \boldsymbol{x}_n^{(t)}$ be the location of n individuals in a region S, $t = 0, 1, \ldots$. We assume that the initial locations, i.e. $\boldsymbol{x}_1^{(0)}, \ldots, \boldsymbol{x}_n^{(0)}$, are uniformly randomly distributed over S. We next assume that a location in S is dominated by the nearest individual. It follows from this assumption that the territory of individual i at time t is given by the Voronoi polygon $V(\boldsymbol{x}_i^{(t)})$ in the Voronoi diagram $\mathcal{V}^{(t)} = \{V(\boldsymbol{x}_1^{(t)}), \ldots, V(\boldsymbol{x}_n^{(t)})\}$. We further assume that individual i moves its location toward the gravitational centre of its territorial area. To be explicit, let $\boldsymbol{u}_{ij}^{(t)} = (u_{ij}^{(t)}, v_{ij}^{(t)})^{\mathrm{T}}$, $j \in I_{n_i}$, be Voronoi vertices of $V(\boldsymbol{x}_i^{(t)})$ which are indexed counterclockwise. Then the gravitational centre, $\boldsymbol{x}_{gi}^{(t)} = (x_{gi}^{(t)}, y_{gi}^{(t)})^{\mathrm{T}}$, of $V(\boldsymbol{x}_i^{(t)})$ is given by

$$
\begin{aligned}
x_{gi}^{(t)} &= \frac{1}{6|V(\boldsymbol{x}_i^{(t)})|} \sum_{j=1}^{n_i} (v_{ij}^{(t)} - v_{j-1}^{(t)}) \left\{ (u_{ij}^{(t)} + u_{ij-1}^{(t)})^2 - u_{ij}^{(t)} u_{ij-1}^{(t)} \right\}, \\
y_{gi}^{(t)} &= \frac{1}{6|V(\boldsymbol{x}_i^{(t)})|} \sum_{j=1}^{n_i} (u_{ij}^{(t)} - u_{j-1}^{(t)}) \left\{ (v_{ij}^{(t)} + v_{ij-1}^{(t)})^2 - v_{ij}^{(t)} v_{ij-1}^{(t)} \right\}.
\end{aligned}
\tag{7.3.6}
$$

In these terms, the above behavioural assumption may be written as follows.

Assumption AP1 (adjustment move)

$$
\boldsymbol{x}_i^{(t+1)} = \boldsymbol{x}_i^{(t)} + \frac{1}{\alpha} \left(\boldsymbol{x}_{gi}^{(t)} - \boldsymbol{x}_i^{(t)} \right), \quad t = 0, 1, 2, \ldots, \tag{7.3.7}
$$

where $\alpha \geq 1$ is a behavioural constant.

We call the process in which all individuals follow Assumption AP1 the *adjustment process* or *adjustment model* (Hasegawa and Tanemura, 1976, 1980, 1986) (Figure 7.3.5). When $\boldsymbol{x}_{gi}^{(t)} = \boldsymbol{x}_i^{(t)}$ for all $i \in I_n$, we say that the configuration of territories is *stable*. If region S is one-dimensional, such as a river side or a beach side, the limiting configuration can be obtained analytically (Hasegawa and Tanemura, 1976; Saito, 1982). In the limit, the configuration becomes stable and all territories become the same size. If region S is two-dimensional, analytical examination is intractable. Hasegawa and Tanemura (1976), employing numerical simulations, concluded from the simulations that the adjustment model leads to a stable configuration and this configuration is fairly close to the configuration of the territories of mouthbreeder fish observed by Barlow (1974) (see Section 7.2).

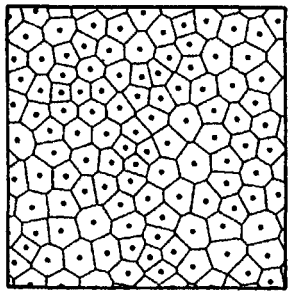

Figure 7.3.5 The adjustment process: ($t = 500$) configuration. (*Source*: Hasegawa and Tanemura, 1981, Figure 1.)

7.4 TWO-SPECIES MODELS

In Section 7.3 we showed the models of territories formed through the interaction within the same kinds of behavioural units. In the real world we also find another type of territories which are formed not only through the interaction within the same kind of behavioural units but also through the interaction between different kinds of behavioural units. In this section we show a few Voronoi-type models that attempt to explain such phenomena.

In animal ecology, many prey–predator relations are known, such as cows and lions, and it is reported that prey tend to form herds or flocks. To explain this tendency, Hamilton (1971) proposes a model which may be called the *selfish herd model*. Consider, as an example, cows and lions in grassland, and suppose that the cows are grazing and the lions are hiding in the grass to catch a cow. Lions tend to catch the cow nearest to their hiding site. Then a Voronoi polygon associated with a cow represents the 'domain of danger' (Hamilton, 1971) of that cow. To be explicit, let $\mathcal{V} = \{V(p_1), \ldots, V(p_n)\}$ be the Voronoi diagram generated by a set of sites of n cows. If a lion happens to be in $V(p_i)$, the cow at p_i will be a prey of the lion. Thus the area of $V(p_i)$ represents the magnitude of danger of the cow at p_i. When a cow senses the presence of a lion, the cow tends to move to the nearest cow. As a result, cows form a herd and each cow wants to be surrounded by the other cows. Actually, the domain of danger of a cow that is tightly surrounded by the other cows becomes small and the cow is less likely to be a prey of a lion. Since every cow wants to be tightly surrounded by the other cows, the configuration of cows within a herd is unstable, but as a whole, a herd guarantees more or less safety. With this model, Hamilton (1971) emphasizes that the selfish avoidance of a predator can lead to aggregation.

The area of a Voronoi polygon has a negative implication for a cow, but it may have a positive implication for certain kinds of insects. As an example Cannings and Cruz Orive (1975) referred to signalling females in relation to mobile males. Consider wingless females scattered over a region. Females send signals to males to be fertilized. Suppose that the intensity of the signal is inversely proportional to the distance from a female and the intensity of the signal is the same for all females. If males respond to the strongest signals and males are distributed fairly uniformly over the region, then the probability of a female being fertilized is proportional to the area of the Voronoi polygon of the female. Each female tries to maximize the probability of being fertilized by moving her location. As a result, the configuration of females changes over time and eventually it may reach an equilibrium configuration. Recalling the profit maximization behaviour in Section 7.3, we notice that this problem is similar to the problem considered in the Hotelling process. Cannings and Cruz Orive (1975) examined whether or not a slight move of a female was profitable provided that the other females were placed on regular hexagonal, square or triangular lattice points. This problem is in fact the same as the problem of the Hotelling process in an unbounded plane,

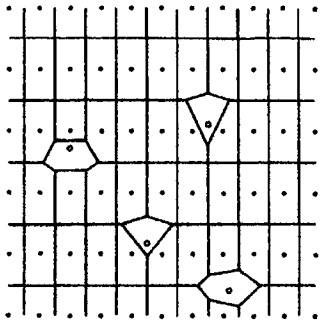

Figure 7.4.1 Two-species model (filled circles indicate crop plants and unfilled circles indicate weeds).

and the answer is shown in Property HP3. This problem is also investigated theoretically by Cruz Orive (1979).

In plant ecology, the prey–predator relationship may correspond to the relationship between crop plants and weeds. This relationship is studied by Fischer and Miles (1973) with a Voronoi diagram. Usually crop plants are planted at rectangular lattice points (the filled circles with $a \times b$ intervals in Figure 7.4.1), whereas weeds are distributed randomly, i.e. the distribution of weeds follows a Poisson process (the unfilled circles in Figure 7.4.1). Suppose that crop plants and weeds emerge simultaneously and expand with equal rates. Ultimately, as we saw in Section 7.2, each plant establishes its individual zone of exploitation, and collectively these form a Voronoi diagram. To estimate the yield of the crop, it is useful to know the expected area $\mu_c(\rho)$ of each crop plant domain (the mean area of each Voronoi polygon) when the density ρ of weeds and intervals a and b are given. Fischer and Miles (1973) obtain this value as

$$\mu_c(\rho) = \frac{4}{\rho} \Psi\left(\sqrt{\frac{\pi\rho}{2}}\, a\right) \Psi\left(\sqrt{\frac{\pi\rho}{2}}\, b\right), \tag{7.4.1}$$

where

$$\Psi(x) = \frac{1}{2\pi} \int_0^x e^{-z^2/2}\, dz. \tag{7.4.2}$$

Fischer and Miles (1973) also examine the cases of simultaneous emergence and different expansion rates, and different emergence and different expansion rates.

We may also find the prey–predator relationship in economic behaviour. Von Hohenbalken and West (1984) and West and Von Hohenbalken (1984) surveyed the entry and withdrawal of stores in Edmonton, Canada, during 1959–1973 to test Kreps and Wilson's (1982) economic predation theory. The predation process assumed by Kreps and Wilson may be summarized as follows.

Suppose that an established firm operates a set of stores in a region and a firm is entering this region with new stores.

(i) The new stores of the entrant are challenged by the neighbourhood stores of the established firm.
(ii) The established firm locates new stores to force losses on the entrant's new stores.
(iii) The entrant stops constructing new stores.
(iv) Eventually, the entrant withdraws from the region.

Von Hohenbalken and West (1984) assume that a set of market areas is represented by a Voronoi diagram and the neighbourhood stores of a store, say store i, are given by stores whose Voronoi polygons are adjacent to the Voronoi polygon of store i. With these assumptions, they investigated empirically the above predation process in Edomonton. They conclude that generally the data support the Kreps and Wilson predation process.